College of Aeronautics Report No. 0402
May 2006

# A Simulation Model of the NFLC Jetstream 31

Dr Alastair K. Cooke
School of Engineering
Cranfield University
Cranfield
Bedford MK43 0AL
a.cooke@cranfield.ac.uk

The opinions expressed herein are those of the author alone and do not necessarily represent those of the University

# A Simulation Model of the NFLC Jetstream 31

College of Aeronautics Report 0402

A review of previous efforts to model NLFC Jetstream 31 was made following a requirement to generate an accurate and comprehensive mathematical representation for incorporation into the Large Flight Simulator (LFS) at Cranfield Univeristy. During the review it became clear that most of the earlier models, having been created for some other more specific purpose, were either incomplete or insufficiently detailed. In addition these models were all based on the recently retired Jetstream Mk1 (G-NLFC) and tended to use the methodology inherent in ESDU data sheets which had also undergone some revision since the last model was created.

It was therefore considered appropriate to revisit the issue and create a new more comprehensive mathematical model of the aircraft using the current suite of ESDU data sheets. The airframe aerodynamics, less powerplant effects, are described in this report.

# Contents

# List of Figures

# List of Tables

# Notation

| | |
|---|---|
| $a_1$ | aerofoil lift-curve slope, $dC_L/d\alpha$, in viscous compressible flow |
| $(a_{1_i})_f$ | fin lift-curve slope in inviscid compressible flow |
| $(a_1)_f$ | fin lift-curve slope in viscous compressible flow |
| $a_{1_i}$ | aerofoil lift-curve slope in inviscid compressible flow |
| $(a_1)_t$ | tailplane lift-curve slope in viscous compressible flow |
| $(a_1)_{ti}$ | isolated tailplane lift-curve slope in viscous compressible flow |
| $(a_{1_i})_t$ | tailplane lift-curve slope in inviscid compressible flow |
| $(a_1)_w$ | wing lift-curve slope in viscous compressible flow |
| $(a_{1_i})_w$ | wing lift-curve slope in inviscid compressible flow |
| $(a_1)_{wb}$ | wing/body lift-curve slope in viscous compressible flow |
| $(a_2)_a$ | aileron lift-curve slope in viscous compressible flow |
| $(a_2)_t$ | elevator lift-curve slope in viscous compressible flow |
| $A$ | aspect ratio |
| $b$ | wing span |
| $c$ | aerofoil chord |
| $\bar{\bar{c}}$ | wing mean aerodynamic chord |
| $\bar{\bar{c}}_f$ | fin mean aerodynamic chord |
| $\bar{\bar{c}}_t$ | tailplane mean aerodynamic chord |
| $c_b$ | propeller blade chord |
| $c_F$ | fin chord at mid-span of rudder |
| $c_r$ | wing root chord |
| $c_{rF}$ | fin root chord - defined by intersection of quarter chord sweep line with body |
| $c_t$ | wing tip chord |
| $c_{tF}$ | fin tip chord |
| $c'$ | extended aerofoil chord |
| $c'_{t1}$ | extended chord of single-slotted trailing edge flap |
| $C_L^*$ | lift coefficient at which flow separation occurs |
| $C_{D0}$ | zero-lift drag coefficient |
| $(C_{Dv})_t$ | lift dependent drag coefficient for tailplane |
| $(C_{Dv})_w$ | lift dependent drag coefficient for wing |
| $C_{L0_{tw}}$ | zero-incidence lift coefficient for a wing with a trailing edge flap deployed |
| $C_{L0_{wb}}$ | zero-incidence lift coefficient for a wing/body combination |
| $C_{L_{wb}}$ | lift coefficient for a wing/body combination |
| $C_{M_0}$ | zero-lift pitching moment in compressible inviscid flow |
| $C_{M_{0_i}}$ | zero-lift pitching moment in incompressible inviscid flow |
| $C_{M_{\alpha 0}}$ | zero-incidence pitching moment in compressible inviscid flow |
| $C_{n_i}$ | yawing moment coefficient due to induced drag from ailerons |
| $C_{n_p}$ | yawing moment coefficient due to profile drag from ailerons |
| $C_S$ | surface area coefficient $4V_f/\pi DL$ |
| $C_V$ | volume coefficient $S/\pi D^2 L$ |

| | |
|---|---|
| $C_{Vf}$ | volume coefficient of forebody $4V_f/\pi D^2 l_f$ |
| $d_{BF}$ | body width at fin root quarter-chord station |
| $D$ | maximum fuselage diameter |
| $D_f$ | skin friction drag |
| $D_0$ | profile drag |
| $D_T$ | tailplane drag |
| $E_T$ | tailplane efficiency, $(a_1)_t \,/\, (a_1)_{ti}$ |
| $F$ | function allowing for effects on sideforce of wing height |
| $F_W$ | function allowing for effects on sideforce of wing planform |
| $h$ | maximum height of fuselage |
| $h+$ | maximum positive camber line ordinate |
| $h_{0.25}$ | position of aero-centre aft of $\bar{\bar{c}}/4$ as a percentage of $\bar{\bar{c}}$ |
| $h_{BF}$ | body height at fin root quarter-chord station |
| $h_F$ | height of fin |
| $h_n$ | maximum height of engine nacelle |
| $h_R$ | spanwise extent of rudder |
| $h_{Ri}$ | height of inboard end of rudder hinge-line above body axes centre |
| $(h_t)_{body}$ | height of tailplane aero-centre above body axes centre |
| $h_V$ | height of ventral fin |
| $i_t$ | tailplane setting angle relative to wing chordline |
| $J_B$ | sideforce correction factor allowing for presence of body |
| $J_R$ | body interference factor |
| $J_{t1}$ | efficiency factor for single-slotted trailing edge flap |
| $J_T$ | sideforce correction factor allowing for presence of tailplane |
| $J_W$ | sideforce correction factor allowing for presence of wing |
| $k_M$ | compressibility correction factor for zero-lift incidence |
| $k_v$ | viscous correction factor for zero-lift incidence |
| $K_B$ | ratio of body lift to exposed wing lift |
| $K$ | nacelle fineness ratio correction factor |
| $K_{B(W)}$ | ratio of change in body lift due to presence of wing to exposed wing lift |
| $K_M$ | secondary Mach factor for tailplane |
| $K_{f0}$ | flap-type correlation factor |
| $K_{W(B)}$ | ratio of wing lift in presence of body to exposed wing lift |
| $l$ | distance of yaw axis behind nose |
| $l_b$ | fuselage length |
| $l_f$ | forebody length |
| $l_R$ | horizontal moment arm of sideforce due to rudder |
| $(l_t)_{body}$ | distance between tailplane aero-centre and body axes centre |
| $l_t$ | distance between wing and tailplane aero-centres |
| $\mathscr{L}$ | rolling moment |
| $L$ | fuselage length |
| $[(L_v)_n]_T$ | theoretical contribution to $L_v$ due to antisymmetric incidence induced by nacelles |
| $L_t$ | tailplane lift |
| $L_p$ | aeronormalised rolling moment derivative due to roll rate, $(\partial\mathscr{L}/\partial p) \,/\, \left(\frac{1}{2}\rho V S_W b^2\right)$ |
| $L_{r0}$ | aeronormalised rolling moment derivative due to yaw rate, incompressible flow |
| $L_r$ | aeronormalised rolling moment derivative due to yaw rate, $(\partial\mathscr{L}/\partial r) \,/\, \left(\frac{1}{2}\rho V S_W b^2\right)$ |
| $L_v$ | aeronormalised rolling moment derivative due to sideslip, $(\partial\mathscr{L}/\partial v) \,/\, \left(\frac{1}{2}\rho V S_W b\right)$ |
| $L_\zeta$ | aeronormalised rolling moment derivative due to rudder, $(\partial\mathscr{L}/\partial\zeta) \,/\, \left(\frac{1}{2}\rho V^2 S_W b\right)$ |
| $L_\xi$ | aeronormalised rolling moment derivative due to aileron, $(\partial\mathscr{L}/\partial\xi) \,/\, \left(\frac{1}{2}\rho V^2 S_W b\right)$ |
| $L_{wb}$ | wing/body lift |
| $m_0$ | distance of engine cowling forward of body axis centre |

| | |
|---|---|
| $m_F$ | distance of fin root quarter-chord behind body axes centre |
| $\mathscr{M}$ | pitching moment |
| $(M_q)_B$ | body pitching moment derivative due to pitch rate, $(\partial\mathscr{M}/\partial q)\ /\ (\frac{1}{2}\rho V S_W \bar{\bar{c}}^2)$ |
| $m_V$ | distance of ventral fin aero-centre behind body axes centre |
| $\mathscr{N}$ | yawing moment |
| $\mathscr{N}_\xi$ | yawing moment arising from aileron deflection |
| $N$ | index to allow for Reynolds number effect on lift curve for wings with flaps deployed |
| $N_p$ | aeronormalised yawing moment derivative due to roll rate, $(\partial\mathscr{N}/\partial p)\ /\ (\frac{1}{2}\rho V S_W b^2)$ |
| $N_r$ | aeronormalised yawing moment derivative due to yaw rate, $(\partial\mathscr{N}/\partial r)\ /\ (\frac{1}{2}\rho V S_W b^2)$ |
| $N_r$ | aeronormalised yawing moment derivative due to yaw rate, $(\partial\mathscr{N}/\partial p)\ /\ (\frac{1}{2}\rho V S_W b^2)$ |
| $N_v$ | aeronormalised yawing moment derivative due to sideslip, $(\partial\mathscr{N}/\partial v)\ /\ (\frac{1}{2}\rho V S_W b)$ |
| $N_\zeta$ | aeronormalised yawing moment derivative due to rudder, $(\partial\mathscr{N}/\partial\zeta)\ /\ (\frac{1}{2}\rho V^2 S_W b)$ |
| $r$ | fuselage radius at wing root |
| $R_e$ | Reynolds number |
| $s$ | wing semispan |
| $S_b$ | fuselage side area |
| $S_f$ | fin area, measured from intersection of quarter chord with fuselage |
| $S_{fus}$ | fuselage cross-sectional area |
| $S_W$ | gross wing area |
| $S_{W_e}$ | exposed wing area |
| $t$ | aerofoil maximum thickness |
| $V$ | velocity of aircraft relative to air |
| $\bar{\bar{x}}_0$ | distance of leading edge of aerodynamic mean chord aft of wing apex |
| $x$ | aerofoil station |
| $x_t$ | chordwise location of maximum thickness |
| $x_{ts}/c$ | chordwise location of flap-shroud trailing edge |
| $\bar{x}_0$ | distance of aerodynamic centre aft of leading edge of root chord |
| $x_T$ | distance of tailplane behind quarter-chord point of wing centreline chord |
| $X_t$ | X-force from tailplane |
| $Y$ | Y-force |
| $Y_p$ | aeronormalised sideforce derivative due to roll rate, $(\partial Y/\partial p)\ /\ (\frac{1}{2}\rho V S_W b)$ |
| $Y_r$ | aeronormalised sideforce derivative due to yaw rate, $(\partial Y/\partial r)\ /\ (\frac{1}{2}\rho V S_W b)$ |
| $Y_v$ | aeronormalised sideforce derivative due to sideslip, $(\partial Y/\partial v)\ /\ (\frac{1}{2}\rho V S_W)$ |
| $Y_\zeta$ | aeronormalised sideforce derivative due to rudder, $(\partial Y/\partial\zeta)\ /\ (\frac{1}{2}\rho V^2 S_W)$ |
| $z$ | vertical position of wing quarter chord below fuselage centre-line |
| $z_0$ | vertical position of nacelle centre-line below body axes centre |
| $z_c$ | aerofoil camber, positive = above chord line |
| $z_{c_2}$ | camber line ordinate at 5.0% chord |
| $z_{c_3}$ | camber line ordinate at 20.0% chord |
| $z_{c_4}$ | camber line ordinate at 50.0% chord |
| $z_{c_5}$ | camber line ordinate at 90.0% chord |
| $z_{c_6}$ | camber line ordinate at 92.0% chord |
| $z_{crF}$ | height of fin root chord above body axes centre |
| $\bar{z}_F$ | height of fin aero-centre above fin root chord |
| $z_R$ | vertical moment arm of sideforce due to rudder |
| $z_t$ | aerofoil thickness, equally distributed above/below camber line |
| $z_{t_1}$ | aerofoil thickness at 0.5% chord |
| $z_{t_2}$ | aerofoil thickness at 5.0% chord |
| $z_B$ | distance of body centreline above wing/body zero lift plane |
| $z_T$ | distance of tailplane above wing/body zero lift plane |
| $z_T$ | height of tailplane above fin root chord |

| | |
|---|---|
| $Z_t$ | Z-force from tailplane |
| $z_V$ | distance of ventral fin aero-centre below body axes centre |
| | |
| $\alpha_0$ | aerofoil zero-lift incidence |
| $(\alpha_0)_T$ | aerofoil zero-lift incidence in inviscid and incompressible flow |
| $(\alpha_0)_w$ | wing zero-lift incidence |
| $(\alpha_0)_{tw}$ | zero-lift incidence for wing/body with trailing edge flap deployed |
| $(\alpha_0)_{wb}$ | wing/body zero-lift incidence |
| $\alpha^*$ | aerofoil incidence at which flow separation occurs |
| $\alpha_b$ | body incidence |
| $\alpha_t$ | tailplane incidence |
| $\alpha_w$ | wing incidence |
| $\Gamma$ | dihedral angle |
| $\delta_f$ | flap rotation angle |
| $\delta_{t1}$ | flap deflection angle |
| $\Delta C'_{D_f}$ | vortex drag coefficient increment due to flap deployment |
| $\Delta C_{D0_f}$ | zero-lift drag coefficient increment due to flap deployment |
| $\Delta C_{L_f}$ | lift coefficient increment due to flap deployment |
| $\bar{\varepsilon}$ | average downwash angle across tailplane |
| $\bar{\varepsilon}_0$ | average downwash angle across tailplane at zero wing/body lift |
| $\bar{\varepsilon}_{fT}$ | average downwash across tailplane with flaps deployed |
| $\eta$ | elevator deflection |
| $\eta_i$ | spanwise location of inboard limit of control surface as a fraction of semi-span |
| $\eta_o$ | spanwise location of outboard limit of control surface as a fraction of semi-span |
| $\lambda$ | profile drag correction factor |
| $\Lambda$ | sweep angle |
| $\eta_t$ | scaling factor for velocity at tailplane |
| $\sigma_e$ | |
| $\sigma_\alpha$ | sidewash factor |
| $\tau_a$ | aerofoil trailing-edge angle |
| $\tau_{au}$ | aerofoil upper surface trailing-edge angle |
| $\Phi_i$ | part-span factor corresponding to $\eta_i$ |
| $\Phi_o$ | part-span factor corresponding to $\eta_o$ |

# Chapter 1

# Lift Estimates

## 1.1 Basic Viscous Flow Estimates

From ESDU 70011 estimates of the lift-curve slope, $a_{1_i}$, and aerodynamic centre location, $\bar{x}_0$, were made for the wing and the tailplane in inviscid flow, see Table 1.1. Note that $\bar{\bar{x}}_0/c_r$ is 0.0843

| | wing | | tailplane | |
|---|---|---|---|---|
| Mach | $(a_{1_i})_w$ rad$^{-1}$ | $\bar{x}_0/c_r$ | $(a_{1_i})_t$ rad$^{-1}$ | $\bar{x}_0/c_r$ |
| 0.05 | 4.955 | 0.261 | 4.262 | 0.349 |
| 0.10 | 4.969 | 0.261 | 4.272 | 0.349 |
| 0.15 | 4.993 | 0.261 | 4.290 | 0.349 |
| 0.20 | 5.028 | 0.261 | 4.315 | 0.349 |
| 0.25 | 5.073 | 0.261 | 4.348 | 0.349 |
| 0.30 | 5.131 | 0.261 | 4.389 | 0.349 |
| 0.35 | 5.204 | 0.261 | 4.439 | 0.348 |
| 0.40 | 5.291 | 0.261 | 4.500 | 0.348 |
| 0.45 | 5.396 | 0.261 | 4.573 | 0.348 |
| 0.50 | 5.521 | 0.261 | 4.660 | 0.348 |
| 0.55 | 5.667 | 0.261 | 4.763 | 0.347 |

Table 1.1: Basic Lift Data (inviscid flow) - Wing and Tailplane

for the wing and 0.170 for the tailplane. The effect of viscosity was determined by evaluating average Reynolds number effects for the constituent aerofoils, see Appendix B. However, as Mach number was one of the key flight condition descriptors, it was necessary to identify typical values of Reynolds number, using ESDU 77021, for flight Mach numbers between 0.05 and 0.55 before these viscous values for lift-curve slope could be calculated, see Table 1.2 and Table 1.3.

| altitude (m) | temperature (K) | pressure (N.m$^{-2}$) | density (kg.m$^{-3}$) | viscosity (N.s.m$^{-2}$) |
|---|---|---|---|---|
| 0 | 288.15 | 101325 | 1.225 | $1.7894\times10^{-5}$ |
| 8000 | 236.15 | 35600 | 0.5253 | $1.5267\times10^{-5}$ |

Table 1.2: Range of Atmospheric Properties

| | sea level | | | | 8000 m | | | |
|---|---|---|---|---|---|---|---|---|
| | wing | | tailplane | | wing | | tailplane | |
| Mach | root | tip | root | tip | root | tip | root | tip |
| 0.05 | 6.408 | 6.301 | 6.291 | 5.902 | 6.066 | 5.958 | 5.949 | 5.560 |
| 0.10 | 6.709 | 6.602 | 6.592 | 6.204 | 6.367 | 6.259 | 6.250 | 5.861 |
| 0.15 | 6.885 | 6.778 | 6.768 | 6.380 | 6.543 | 6.436 | 6.426 | 6.038 |
| 0.20 | 7.010 | 6.903 | 6.893 | 6.505 | 6.668 | 6.561 | 6.551 | 6.162 |
| 0.25 | 7.107 | 7.000 | 6.990 | 6.601 | 6.765 | 6.657 | 6.648 | 6.259 |
| 0.30 | 7.186 | 7.079 | 7.069 | 6.681 | 6.844 | 6.737 | 6.727 | 6.339 |
| 0.35 | 7.253 | 7.146 | 7.136 | 6.748 | 6.911 | 6.804 | 6.794 | 6.405 |
| 0.40 | 7.311 | 7.204 | 7.194 | 6.806 | 6.969 | 6.862 | 6.852 | 6.463 |
| 0.45 | 7.362 | 7.255 | 7.245 | 6.857 | 7.020 | 6.913 | 6.903 | 6.515 |
| 0.50 | 7.408 | 7.301 | 7.291 | 6.902 | 7.066 | 6.958 | 6.949 | 6.560 |
| 0.55 | 7.449 | 7.342 | 7.332 | 6.944 | 7.107 | 7.000 | 6.990 | 6.602 |

Table 1.3: Range of Reynolds Numbers - $\log_{10}(R_e)$

The Reynolds numbers were averaged and used to estimate the lift-curve slope reduction factor, $a_1/a_{1_i}$, for each aerofoil section, see Appendix B. The viscous factors were then averaged to yield values of lift-curve slope suitable for the wing and tailplane, see Table 1.4. The tailplane values were further reduced by 4% to account for the elevator cutout in accordance with ESDU Aero W.01.01.04.

| | wing | | tailplane | |
|---|---|---|---|---|
| Mach | $(a_1)_w$ rad$^{-1}$ | $\bar{x}_0/c_r$ | $(a_1)_{ti}$ rad$^{-1}$ | $\bar{x}_0/c_r$ |
| 0.05 | 4.537 | 0.261 | 3.783 | 0.349 |
| 0.10 | 4.601 | 0.261 | 3.827 | 0.349 |
| 0.15 | 4.652 | 0.261 | 3.863 | 0.349 |
| 0.20 | 4.702 | 0.261 | 3.897 | 0.349 |
| 0.25 | 4.754 | 0.261 | 3.933 | 0.349 |
| 0.30 | 4.815 | 0.261 | 3.975 | 0.349 |
| 0.35 | 4.884 | 0.261 | 4.023 | 0.348 |
| 0.40 | 4.963 | 0.261 | 4.079 | 0.348 |
| 0.45 | 5.054 | 0.261 | 4.141 | 0.348 |
| 0.50 | 5.160 | 0.261 | 4.216 | 0.348 |
| 0.55 | 5.266 | 0.261 | 4.303 | 0.347 |

Table 1.4: Basic Lift Data (viscous flow) - Wing and Tailplane

## 1.2 Wing and Body Lift

The Jetstream 31 configuration places a large forebody in front of the mainplane thereby modifying the flow over the inboard sections of the wing and leading to an increase in lift. From ESDU 91007:

$$(a_1)_{wb} = (a_1)_w \left[K_B + K_{W(B)} + K_{B(W)}\right] \frac{S_{W_e}}{S_W}$$

Where:

$$K_B = \frac{2\pi r^2}{S_{W_e}\,(a_{1_i})_w} \qquad K_{W(B)} + K_{B(W)} = \left(1 + \frac{r}{s}\right)^2 = 1.266$$

In addition, from ESDU 90010, the presence of the fuselage shifts the wing aero-centre rearwards by a small amount ($\Delta x_{ac}$), see Table 1.5.

| Mach | $(a_1)_w$ rad$^{-1}$ | $K_B$ | $(a_1)_{wb}$ rad$^{-1}$ | $\Delta x_{ac}/c_r$ |
|---|---|---|---|---|
| 0.05 | 4.537 | 0.0594 | 5.011 | 0.013 |
| 0.10 | 4.601 | 0.0593 | 5.081 | 0.013 |
| 0.15 | 4.652 | 0.0590 | 5.137 | 0.013 |
| 0.20 | 4.702 | 0.0586 | 5.190 | 0.013 |
| 0.25 | 4.754 | 0.0580 | 5.245 | 0.013 |
| 0.30 | 4.815 | 0.0574 | 5.310 | 0.013 |
| 0.35 | 4.884 | 0.0566 | 5.383 | 0.013 |
| 0.40 | 4.963 | 0.0556 | 5.466 | 0.013 |
| 0.45 | 5.054 | 0.0546 | 5.562 | 0.013 |
| 0.50 | 5.160 | 0.0533 | 5.673 | 0.013 |
| 0.55 | 5.266 | 0.0520 | 5.783 | 0.013 |

Table 1.5: Lift Data - Wing and Body

The zero lift angle of attack of the wing/body combination was determined from Appendix B using ESDU 87031 and ESDU 89042. It was assumed that the similarity of the camber profile between the wing root and tip meant that only the effect of the washout need be considered.

| Mach | $(\alpha_0)_{wb}$ rad |
|---|---|
| 0.05 | -0.03407 |
| 0.10 | -0.03515 |
| 0.15 | -0.03566 |
| 0.20 | -0.03604 |
| 0.25 | -0.03624 |
| 0.30 | -0.03632 |
| 0.35 | -0.03637 |
| 0.40 | -0.03639 |
| 0.45 | -0.03636 |
| 0.50 | -0.03617 |
| 0.55 | -0.03585 |

Table 1.6: Zero Lift Incidence - Wing and Body

## 1.3 Effect of Flaps

The Jetstream 31 has three in-flight flap positions 10°, 20° and 35°. From Figures 1.1 and A.1 the various flap parameters for use with ESDU[1] were determined, see Table 1.7. Given that

[1]It was decided to treat the flap as single-slotted due to the presence of a flap shroud on the lower wing surface and the small degree of penetration of the second flap element into the flow field.

$\bar{\eta} = 0.42$, from ESDU 83040, and that from ESDU 97003 $\eta_i = 0.09$ and $\eta_o = 0.60$, then from ESDU 93019:

$$\Phi_i = 0.12 \qquad \Phi_o = 0.73 \qquad K_{f0} = 1.05$$

and:

$$\Delta C_{L0_{tw}} = \left(\frac{c'}{c}\right) K_{f0} J_{t1} \Delta C'_{L1} \left[\frac{(a_1)_w}{2\pi}\right] (\Phi_o - \Phi_i)$$

Where $\Delta C'_{L1} = 0.56$, 0.86 and 1.14 respectively for flap settings 10°, 20° and 35°. The zero incidence lift increments arising from flap deployment were estimated using ESDU 93019. These were added to the lift estimates for the basic wing/body combination and used, along with ESDU 96003, to determine corresponding values for the zero-lift angle of attack, see Table 1.8.

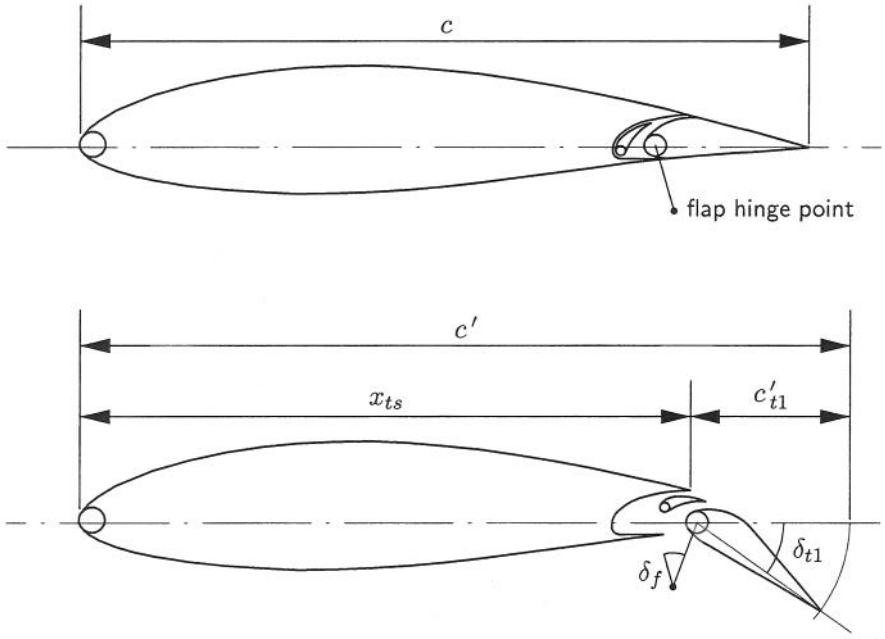


Figure 1.1: Flap Deflections and Parameters

| flap setting ($\delta_f$) | 10° | 20° | 35° |
|---|---|---|---|
| $\delta_{t1}$ | 11.5 | 21.8 | 35.7 |
| $x_{ts}/c$ | 0.8375 | 0.8375 | 0.8375 |
| $c'_{t1}/c$ | 0.179 | 0.195 | 0.220 |
| $c'/c$ | 1.016 | 1.033 | 1.058 |
| $\delta c_t/c$ | 0.016 | 0.033 | 0.058 |
| $K_\delta c_t/c$ | 0.0046 | 0.0163 | 0.0428 |
| $J_{t1}$ | 0.975 | 1.165 | 1.170 |

Table 1.7: Flap Parameters

To ensure that the simulation was constrained to linear aerodynamics, the lift characteristics at the onset of flow separation were determined using ESDU 84026, ESDU 87031, ESDU 89034 and

| | Mach | 0.05 | 0.10 | 0.15 | 0.20 | 0.25 |
|---|---|---|---|---|---|---|
| | N | 0.835 | 0.735 | 0.670 | 0.610 | 0.570 |
| flap setting ($\delta_f$) | $C_{L0_{wb}}$ | 0.171 | 0.179 | 0.183 | 0.187 | 0.190 |
| 10° | $\Delta C_{L0_{tw}}$ | 0.280 | 0.281 | 0.282 | 0.284 | 0.287 |
| | $C_{L0_{tw}}$ | 0.451 | 0.460 | 0.465 | 0.471 | 0.477 |
| | $(\alpha_0)_{tw}$ rad | -0.0907 | -0.0921 | -0.0928 | -0.0933 | -0.0936 |
| 20° | $\Delta C_{L0_{tw}}$ | 0.523 | 0.524 | 0.527 | 0.530 | 0.535 |
| | $C_{L0_{tw}}$ | 0.693 | 0.703 | 0.710 | 0.717 | 0.725 |
| | $(\alpha_0)_{tw}$ rad | -0.1397 | -0.1410 | -0.1417 | -0.1421 | -0.1423 |
| 35° | $\Delta C_{L0_{tw}}$ | 0.713 | 0.715 | 0.718 | 0.723 | 0.729 |
| | $C_{L0_{tw}}$ | 0.883 | 0.893 | 0.901 | 0.910 | 0.920 |
| | $(\alpha_0)_{tw}$ rad | -0.1790 | -0.1803 | -0.1808 | -0.1812 | -0.1813 |

Table 1.8: Zero-lift Incidence due to Flap Deflection

ESDU 91014, see Table 1.9. As a result wing/body lift, for angles of attack up to and including $\alpha^*$, is given by:

$$L_{wb} = \frac{1}{2}\rho V_0^2 S_W C_{L_{wb}} = \bar{q} S_w C_{L_{wb}}$$

Where for the clean wing:

$$C_{L_{wb}} = (a_1)_{wb}\left[\alpha_w - (\alpha_0)_w\right] = (a_1)_{wb}\left[\alpha_b + 1° - (\alpha_0)_w\right]$$

and for the wing with flaps deployed:

$$C_{L_{wb}} = (a_1)_w \left[1 + (\Phi_0 - \Phi_i)\left\{\frac{\delta c_t}{c} - \frac{K_\delta c_t}{c}\right\}\right]\left[\alpha_w - (\alpha_0)_{tw}\right]\cos^N\left[\alpha_w - (\alpha_0)_{tw}\right]$$

given the parameters listed in Table 1.8.

| | Mach | | | | | | | |
|---|---|---|---|---|---|---|---|---|
| flap setting($\delta_f$) | 0.05 | 0.10 | 0.15 | 0.20 | 0.25 | 0.30 | 0.35 | 0.40 |
| 0° | 0.2115 | 0.2114 | 0.2106 | 0.1904 | 0.1747 | 0.1570 | 0.1434 | 0.1319 |
| 10° | 0.2275 | 0.2311 | 0.2322 | 0.2119 | 0.1960 | - | - | - |
| 20° | 0.2115 | 0.2163 | 0.2179 | 0.1972 | 0.1810 | - | - | - |
| 35° | 0.2140 | 0.2201 | 0.2222 | 0.2007 | 0.1839 | - | - | - |

Table 1.9: Onset of Flow Separation - $\alpha^*$ rad

Figures 1.2 and 1.3 give examples of the the variation of predicted wing/body lift with Mach number and flap setting.

## 1.4 Tailplane Lift

The lift produced by a symmetric tailplane is given by:

$$L_t = \frac{1}{2}\rho V_t^2 S_t C_{L_t} = \eta_t \bar{q} S_t C_{L_t}$$

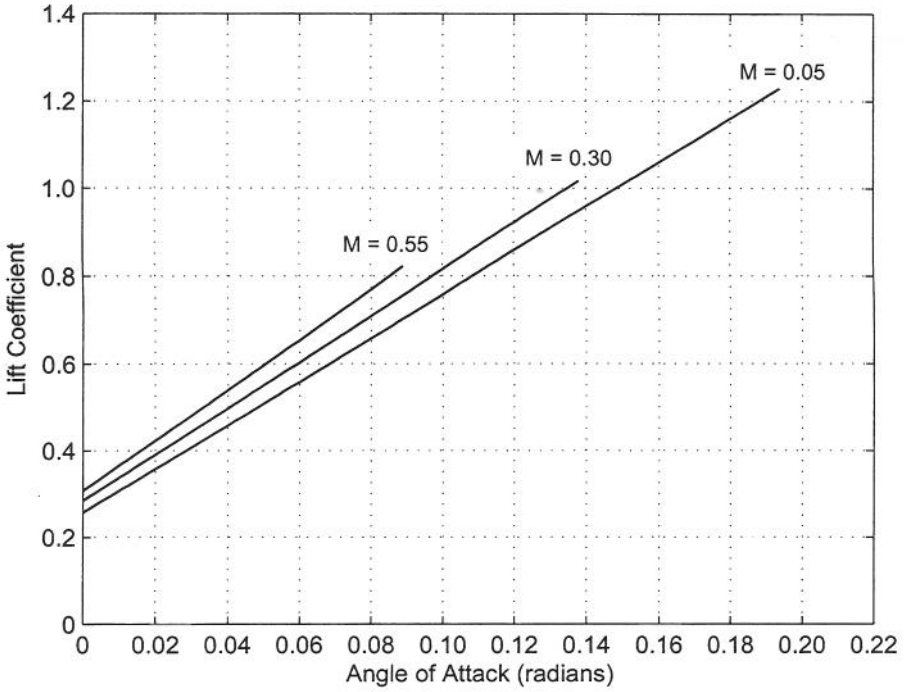


Figure 1.2: Variation of Wing and Body Lift Coefficient with Mach Number

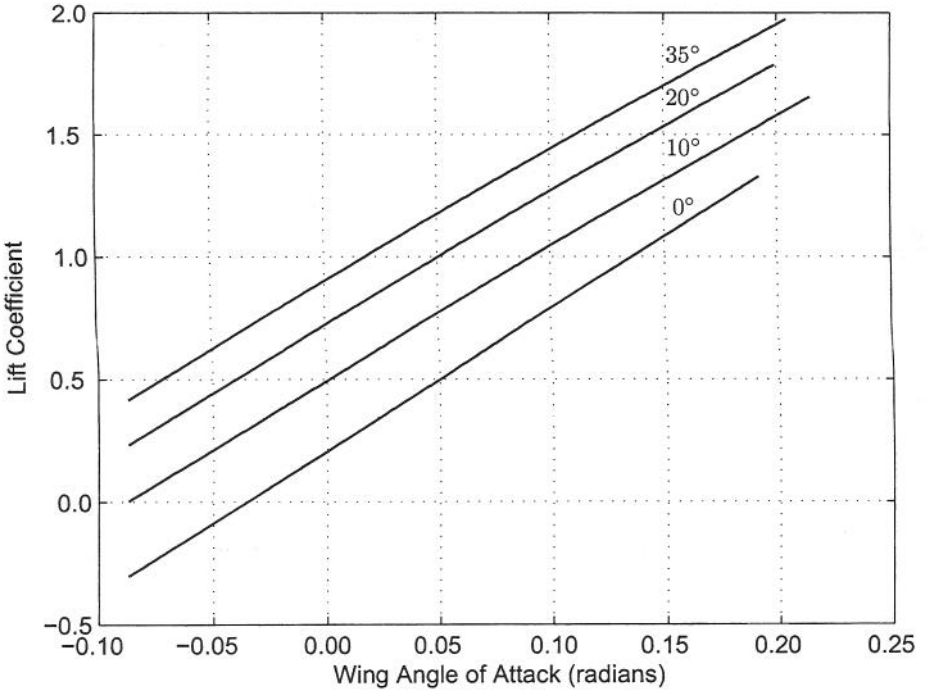


Figure 1.3: Variation of Wing and Body Lift Coefficient with Flap Angle at M = 0.15

where from ESDU 80020:

$$\begin{aligned} C_{L_t} &= (a_1)_t\,\alpha_t + (a_2)_t\,\eta = (a_1)_t\,\{\alpha_w - \bar{\varepsilon} + i_t\} + (a_2)_t\,\eta \\ &= (a_1)_t\left[\alpha_w - \bar{\varepsilon}_0 - \frac{d\bar{\varepsilon}}{d\alpha}\{\alpha_w - (\alpha_0)_{wb}\} + i_t\right] + (a_2)_t\,\eta \end{aligned}$$

Now ESDU 89029 suggests that the presence of the fuselage has an effect of the tailplane lift curve slope:

$$(a_1)_t = K_M E_T\,(a_1)_{ti}$$

Where $E_T$ is equal to 0.82, see Table 1.10 for $(a_1)_t$. From Figures A.2 and A.3 the following geometrical parameters were determined:

$$\begin{aligned} \eta_T &= \frac{s_T}{s} = 0.417 \\ \xi_T &= \frac{x_T}{s} = 0.773 \\ \zeta_T &= \frac{z_T}{s} = 0.350 \\ \zeta_B &= \frac{z_B}{s} = 0.179 \end{aligned}$$

Using ESDU 80020 gives $\varepsilon_0 = 0.0349$ rad, see Table 1.10 for $d\bar{\varepsilon}/d\alpha$. The rate of change of lift coefficient with control deflection was estimated from ESDU 74011, see also Table 1.10 and Figure 1.4.

| Mach | $d\bar{\varepsilon}/d\alpha$ | $K_M$ | $(a_1)_t$ rad$^{-1}$ | $(a_2)_t$ rad$^{-1}$ |
|---|---|---|---|---|
| 0.05 | 0.2763 | 1.000 | 3.102 | 2.339 |
| 0.10 | 0.2763 | 1.000 | 3.138 | 2.368 |
| 0.15 | 0.2763 | 1.000 | 3.168 | 2.391 |
| 0.20 | 0.2763 | 1.000 | 3.196 | 2.414 |
| 0.25 | 0.2763 | 0.998 | 3.217 | 2.438 |
| 0.30 | 0.2763 | 0.995 | 3.244 | 2.467 |
| 0.35 | 0.2769 | 0.990 | 3.266 | 2.500 |
| 0.40 | 0.2780 | 0.985 | 3.294 | 2.539 |
| 0.45 | 0.2799 | 0.978 | 3.320 | 2.583 |
| 0.50 | 0.2824 | 0.965 | 3.336 | 2.636 |
| 0.55 | 0.2860 | 0.955 | 3.369 | 2.698 |

Table 1.10: Downwash at Tailplane and Modified Lift Curve Slopes

The effect of flap defection on the downwash at the tailplane was estimated using ESDU 97021, see Table 1.11. Figure 1.5 shows the resulting effect on the tailplane lift coefficient at neutral elevator.

## 1.5 Effect of Pitch Rate and Vertical Acceleration on Incidence

Pitch rate, $q$, and vertical acceleration, $\dot{w}$, were used to determine the local upwash at the wing or tail aero-centre from which a modified angle of attack and total velocity were estimated. See Figure 1.6, where:

$$\alpha_{\dot{w}} = \frac{d\bar{\varepsilon}}{d\alpha} \cdot \frac{\dot{w} l_{ta}}{V^2}$$

and $l_{ta}$ is the distance between the wing and tailplane aero-centres.

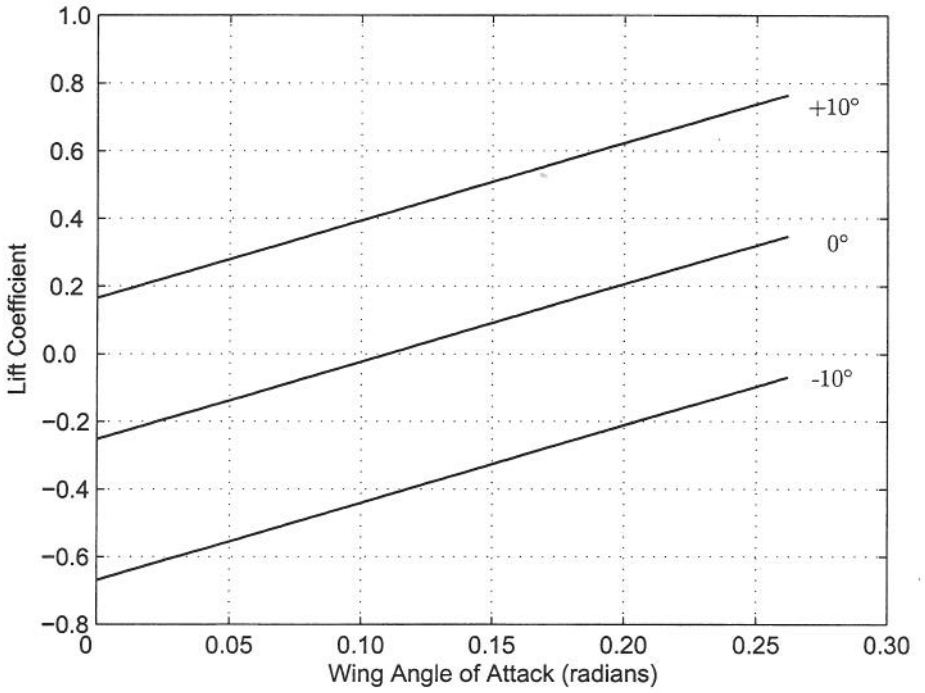


Figure 1.4: Variation of Tailplane Lift Coefficient with Elevator Deflection at M = 0.15

| $\alpha_b$ (deg) | -5 | 0 | 5 | 10 | |
|---|---|---|---|---|---|
| $\alpha_w$ (rad) | -0.06981 | 0.01745 | 0.10472 | 0.19199 | |
| flap setting ($\delta_f$) | | $\bar{\varepsilon}_{fT}$ rad | | | Mach |
| 10° | 0.00804 | 0.04114 | 0.07290 | 0.10301 | 0.05 |
| | 0.00859 | 0.04172 | 0.07356 | 0.10381 | 0.10 |
| | 0.00890 | 0.04215 | 0.07410 | 0.10449 | 0.15 |
| | 0.00915 | 0.04259 | 0.07471 | 0.10525 | 0.20 |
| | 0.00935 | 0.04303 | 0.07535 | 0.10605 | 0.25 |
| 20° | 0.02556 | 0.05648 | 0.08584 | 0.11356 | 0.05 |
| | 0.02608 | 0.05705 | 0.08651 | 0.11438 | 0.10 |
| | 0.02643 | 0.05751 | 0.08709 | 0.11509 | 0.15 |
| | 0.02674 | 0.05799 | 0.08772 | 0.11586 | 0.20 |
| | 0.02703 | 0.05850 | 0.08839 | 0.11666 | 0.25 |
| 35° | 0.03807 | 0.06710 | 0.09451 | 0.12040 | 0.05 |
| | 0.03858 | 0.06767 | 0.09520 | 0.12125 | 0.10 |
| | 0.03891 | 0.06812 | 0.09577 | 0.12195 | 0.15 |
| | 0.03928 | 0.06864 | 0.09644 | 0.12274 | 0.20 |
| | 0.03962 | 0.06918 | 0.09711 | 0.12350 | 0.25 |

Table 1.11: Effect of Flap Deflection on Downwash at Tailplane

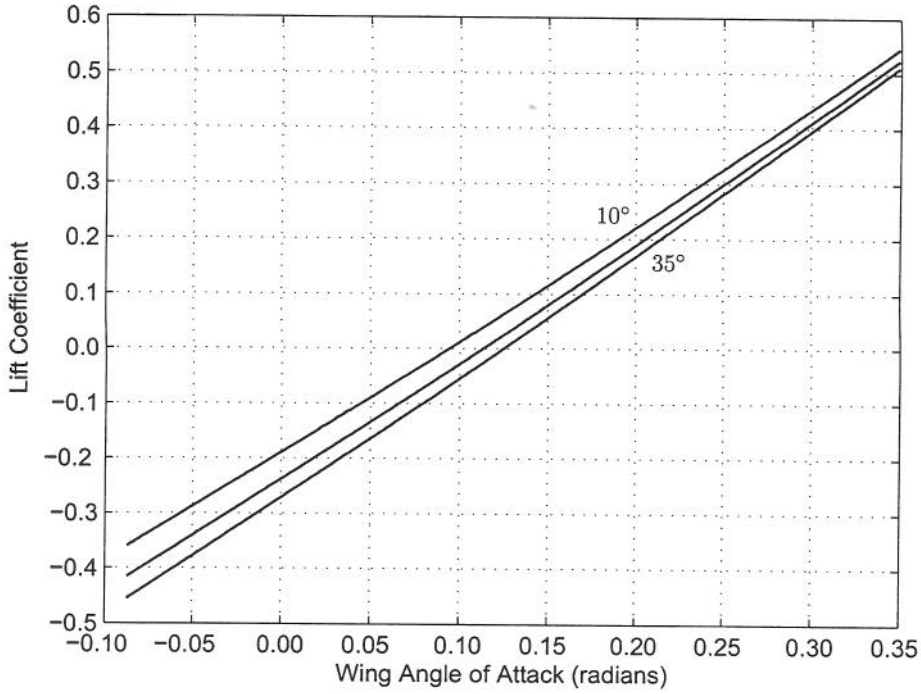


Figure 1.5: Variation of Tailplane Lift Coefficient with Flap Deflection at M = 0.15

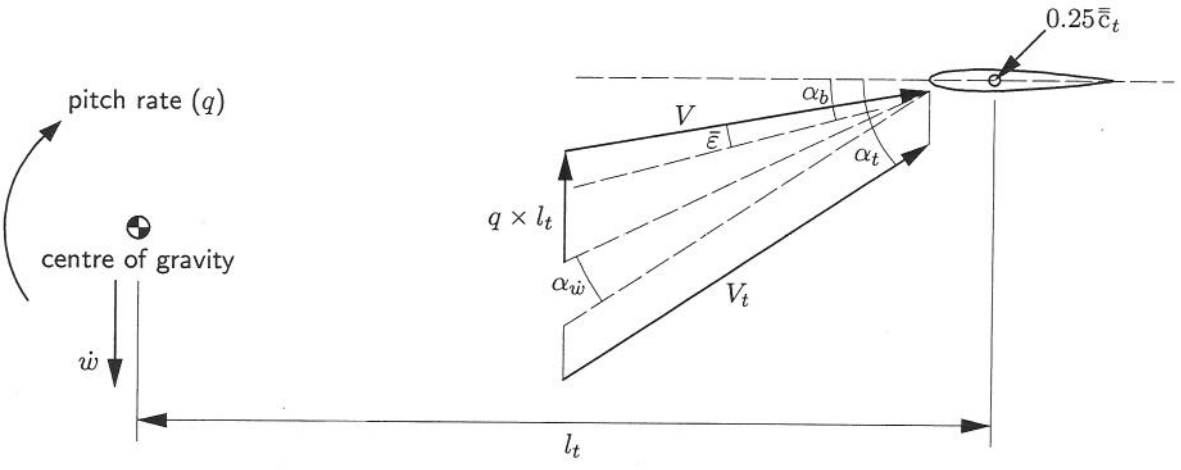


Figure 1.6: Effect of Pitch Rate and Changes in Vertical Velocity on Tailplane Incidence

# Chapter 2

# Drag Estimates

## 2.1 Profile Drag

Profile drag comprising form drag and skin friction drag was determined for the wing, tailplane and fin using McCormick [1979] and ESDU Aero W.02.04.02. Assuming that the wetted area is twice planform area gives:

$$S_{wet_w} = 41.881 \text{ m}^2 \qquad S_{wet_t} = 15.268 \text{ m}^2 \qquad S_{wet_f} = 10.821 \text{ m}^2$$

Now, from McCormick [1979], assuming transition at the leading edge:

$$C_f = \frac{D_f}{\bar{q} S_{wet}} = 0.455 \left(\log_{10} R_e\right)^{-2.58}$$

Where the average Reynolds number is given in Table 2.1.

| Mach | Wing | Tailplane | Fin |
|---|---|---|---|
| 0.05 | 6.017 | 5.927 | 6.079 |
| 0.10 | 6.318 | 6.228 | 6.380 |
| 0.15 | 6.494 | 6.404 | 6.556 |
| 0.20 | 6.619 | 6.529 | 6.681 |
| 0.25 | 6.716 | 6.626 | 6.778 |
| 0.30 | 6.795 | 6.705 | 6.857 |
| 0.35 | 6.862 | 6.772 | 6.924 |
| 0.40 | 6.920 | 6.830 | 6.982 |
| 0.45 | 6.971 | 6.882 | 7.033 |
| 0.50 | 7.017 | 6.927 | 7.079 |
| 0.55 | 7.059 | 6.969 | 7.120 |

Table 2.1: Average Reynolds Numbers - $\log_{10}(R_e)$

As $D_f = \bar{q} S_{wet} C_f = \bar{q} S_{plan} C_{D0}$ and $S_{wet} = 2 S_{plan}$ then $C_{D0} = 2 C_f$. Profile drag correction factors, $\lambda$, based on the mean aerofoil section were estimated, from ESDU Aero W.02.04.02, as $\lambda_w = 1.51$ and $\lambda_t = \lambda_f = 1.36$. Hence the profile drag is given by:

$$D_0 = \bar{q} S_{plan} \lambda C_{D0} = \bar{q} S_{wet} \lambda C_f$$

The effect of deployment of the control surfaces on the profile drag[1] was determined from ESDU 87024 and ESDU Aero F.02.01.07, see Table 2.2. Flap increments were estimated as 0.0031,

| deflection (deg) | deflection (rad) | elevator | rudder | aileron |
|---|---|---|---|---|
| -20 | -0.3491 | 0.0385 | 0.0248 | 0.0032 |
| -15 | -0.2618 | 0.0226 | 0.0146 | 0.0012 |
| -10 | -0.1745 | 0.0104 | 0.0067 | -0.0001 |
| -5 | -0.0873 | 0.0026 | 0.0017 | -0.0005 |
| 0 | 0.0000 | 0.0000 | 0.0000 | 0.0000 |
| 5 | 0.0873 | 0.0026 | 0.0017 | 0.0015 |
| 10 | 0.1745 | 0.0104 | 0.0067 | 0.0038 |
| 15 | 0.2618 | 0.0226 | 0.0146 | 0.0067 |
| 20 | 0.3491 | 0.0385 | 0.0248 | 0.0101 |
| 25 | 0.4363 | 0.0567 | 0.0366 | 0.0137 |
| 30 | 0.5236 | 0.0758 | 0.0489 | 0.0172 |

Table 2.2: Profile Drag Coefficient Increment Due to Control Deflection

0.0105 and 0.0283 for 10°, 20° and 35° respectively using ESDU 87005. Having simplified the fuselage to an axisymmetric shape with the following properties, using ESDU 77028, the profile drag of the fuselage was found from ESDU 78019.

$$\frac{D}{L} = 0.1526 \qquad C_{Vf} = 0.6433 \qquad \frac{l_f}{L} = 0.2778 \qquad C_S = 0.7082 \qquad C_V = 0.7971$$

Hence:

$$(D_0)_{fus} = (C_D)_{fus}\, \bar{q} \pi D L C_S$$

Where $(C_D)_{fus}$ is given in Table 2.3

| Mach | $C_F$ | $(C_D)_{fus}$ |
|---|---|---|
| 0.05 | 0.002699 | 0.00385 |
| 0.10 | 0.002415 | 0.00345 |
| 0.15 | 0.002267 | 0.00324 |
| 0.20 | 0.002168 | 0.00310 |
| 0.25 | 0.002094 | 0.00300 |
| 0.30 | 0.002035 | 0.00292 |
| 0.35 | 0.001985 | 0.00285 |
| 0.40 | 0.001941 | 0.00279 |
| 0.45 | 0.001903 | 0.00274 |
| 0.50 | 0.001867 | 0.00269 |
| 0.55 | 0.001835 | 0.00265 |

Table 2.3: Variation of Surface Area-based Profile Drag Coefficient for Body

[1]To account for non-symmetric deflection the increments given for the aileron are per surface

## 2.2 Lift Dependent or Vortex Drag

From ESDU 66032 and ESDU 74035 the lift dependent drag of the tailplane is given by:

$$(C_{Dv})_t = \left[\frac{1+\delta+\pi A K_1}{\pi A}\right] C_L^2$$

Where $(1+\delta)$ and $K_1$ are shown in Table 2.4. From ESDU 97002 the vortex drag of the wing

| Mach | $K_1$ | $(1+\delta)$ |
|---|---|---|
| 0.05 | 0.00431 | 1.00286 |
| 0.10 | 0.00377 | 1.00284 |
| 0.15 | 0.00347 | 1.00280 |
| 0.20 | 0.00328 | 1.00275 |
| 0.25 | 0.00318 | 1.00268 |
| 0.30 | 0.00307 | 1.00260 |
| 0.35 | 0.00300 | 1.00250 |
| 0.40 | 0.00296 | 1.00239 |
| 0.45 | 0.00295 | 1.00225 |
| 0.50 | 0.00295 | 1.00210 |
| 0.55 | 0.00296 | 1.00192 |

Table 2.4: Variation of Lift Dependent Drag Factors for Tailplane

is given by:

$$(C_{Dv})_w = \frac{1}{\pi A}\left[k_1 C_{L1}^2 + k_f \Delta C_{L0_{tw}}^2 + k_{1f} C_{L1} \Delta C_{L0_{tw}}\right]$$

where $C_{L1}$ represents the lift coefficient due to incidence, camber and twist and $\Delta C_{L0_{tw}}$ is shown in Table 1.8, see also Tables 2.5 and 2.6. From Table 2.5 it can be seen that $k_1$ and $k_{1f}$ are essentially constant with flap angle. The value of $k_1$ for the plain wing was found using ESDU 01007 and is shown in Table 2.7. The relatively low incidence anticipated for cruising flight suggested a slightly different approach. Rather making $k_1$ a function of $a_w$ it was decided to use a constant value based on a mid-range angle of attack (6°). Illustrative whole aircraft drag

| | 10° | | 20° | | 35° | |
|---|---|---|---|---|---|---|
| Incidence | $k_1$ | $k_{1f}$ | $k_1$ | $k_{1f}$ | $k_1$ | $k_{1f}$ |
| 0° | 1.068 | 2.141 | 1.068 | 2.141 | 1.068 | 2.142 |
| 2° | 1.041 | 2.095 | 1.041 | 2.095 | 1.041 | 2.095 |
| 4° | 1.030 | 2.072 | 1.030 | 2.072 | 1.030 | 2.072 |
| 6° | 1.024 | 2.058 | 1.024 | 2.058 | 1.024 | 2.058 |
| 8° | 1.021 | 2.048 | 1.021 | 2.049 | 1.021 | 2.049 |
| 10° | 1.018 | 2.042 | 1.018 | 2.042 | 1.018 | 2.042 |
| 12° | 1.017 | 2.037 | 1.017 | 2.037 | 1.017 | 2.037 |

Table 2.5: Variation of Vortex Drag Factors with Incidence - Flaps Deployed

polars are shown in Figure 2.1

| Mach | 10° | 20° | 35° |
|---|---|---|---|
| 0.05 | 2.021 | 2.024 | 2.036 |
| 0.10 | 2.018 | 2.021 | 2.034 |
| 0.15 | 2.014 | 2.017 | 2.029 |
| 0.20 | 2.008 | 2.011 | 2.023 |
| 0.25 | 2.000 | 2.003 | 2.016 |

Table 2.6: Variation of Vortex Drag Factor ($k_f$) with Mach Number - Flaps Deployed

| Mach | 0.05 | 0.10 | 0.15 | 0.20 | 0.25 | 0.30 | 0.35 | 0.40 | 0.45 | 0.50 | 0.55 |
|---|---|---|---|---|---|---|---|---|---|---|---|
| $k_1$ | 1.024 | 1.024 | 1.024 | 1.024 | 1.024 | 1.023 | 1.023 | 1.022 | 1.022 | 1.021 | 1.021 |

Table 2.7: Variation of Vortex Drag Factor ($k_1$) with Mach Number - Clean Wing

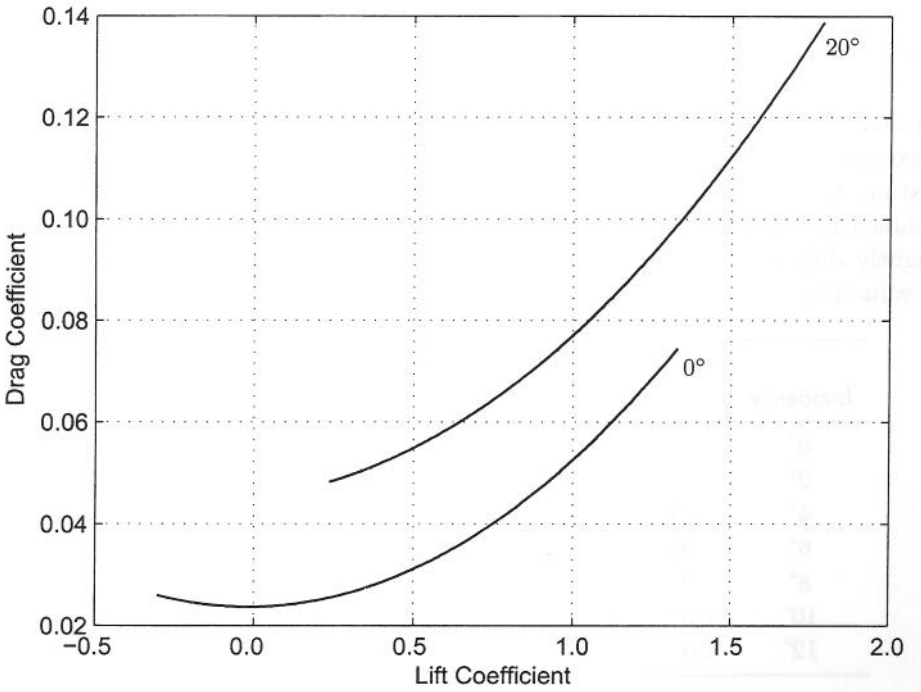


Figure 2.1: Drag Polars - M = 0.15 (Clean and Flaps at 20°)

# Chapter 3

# Pitching Moment Estimates

The total aircraft pitching moment arises from the combined effect of the wing/body combination, the tailplane and the propellers. Estimates for the propeller are not covered in this report. Contributions from the airframe are from two sources: lift and drag forces acting away from the centre of gravity and zero-lift pitching moments. Moments arising from component lift and drag were referenced to the body axes centre using the methodology described in Figure 3.1

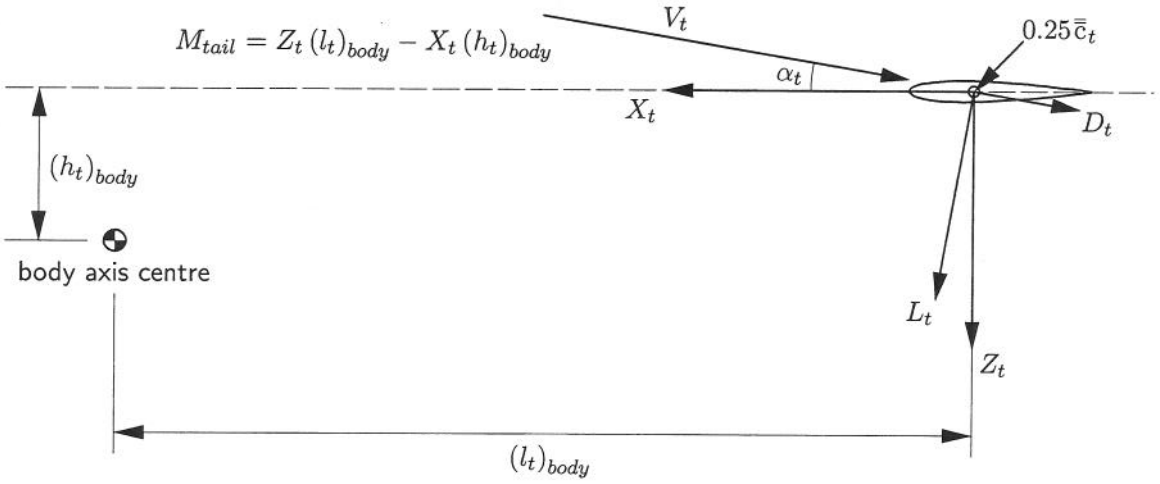


Figure 3.1: Moments Arising from Tailplane Lift and Drag

Now the pitching moment coefficient about the quarter mean aerodynamic chord for the basic wing/body combination at any angle of attack is given by:

$$C_{M_{wb}} = C_{M_0} - h_{0.25}C_{L_{wb}} = C_{M_0} - h_{0.25}\left(C_{L0_{wb}} + \Delta C_{L_{wb}}\right) = C_{M_{\alpha 0}} - h_{0.25}\left(C_L - C_{L0_{wb}}\right)$$

Where $C_{L0_{wb}}$ is the wing lift produced at zero angle of attack and $C_{M_{\alpha 0}}$ is the pitching moment developed at the same condition. With flap deployed the wing camber is increased and the aero-centre moves aft, so:

$$C_{M_{tw}} = C_{M_{0tw}} - \left(h_{0.25} + \Delta h_1\right) C_{L_{tw}}$$

Or

$$C_{M_{tw}} = C_{M_{\alpha 0}} + \Delta C_{M_{\alpha 0}} - \left(h_{0.25} + \Delta h_1\right)\left(C_L - C_{L0_{tw}}\right)$$

The zero-lift pitching moment for the clean wing was determined from ESDU 87001 using the section values for $C_{M_0}$ given in Appendix B and assuming a linear variation between root and

tip, see Table 3.1. The effect of flap deflection was estimated using ESDU 03017 and ESDU 99004, thus[1] $C_{M_{\alpha 0}}$ is given in Table 3.1 and $\Delta h_1$ is given in Table 3.2. As the tailplane has a symmetric aerofoil section the pitching moment coefficient about the quarter mean aerodynamic chord of the tailplane is given by:

$$C_{M_t} = -h_{0.25_t} (a_1)_t \alpha_t - k_f h_2 (a_2)_t |\eta| = -h_{0.25_t} (a_1)_t \alpha_t - k_f m_0 |\eta|$$

Using the two-dimensional section data from ESDU Aero C.08.01.01 and converting it to three-dimensional 'wing' data using ESDU 98017 it was found that $m_0$ is 0.652 and $k_f$ is as given in Table 3.1. Figures 3.2 show the variation of wing-referenced pitching moment coefficient with flap and elevator deflection[2]. Pitching moments arising from pitch rate ($q$) and rate of change of vertical velocity, ($\dot{w}$), have already been determined by the modifications to wing and tail angle of attack described above. The fuselage contribution to $M_q$ was estimated using ESDU 90010, see Table 3.1.

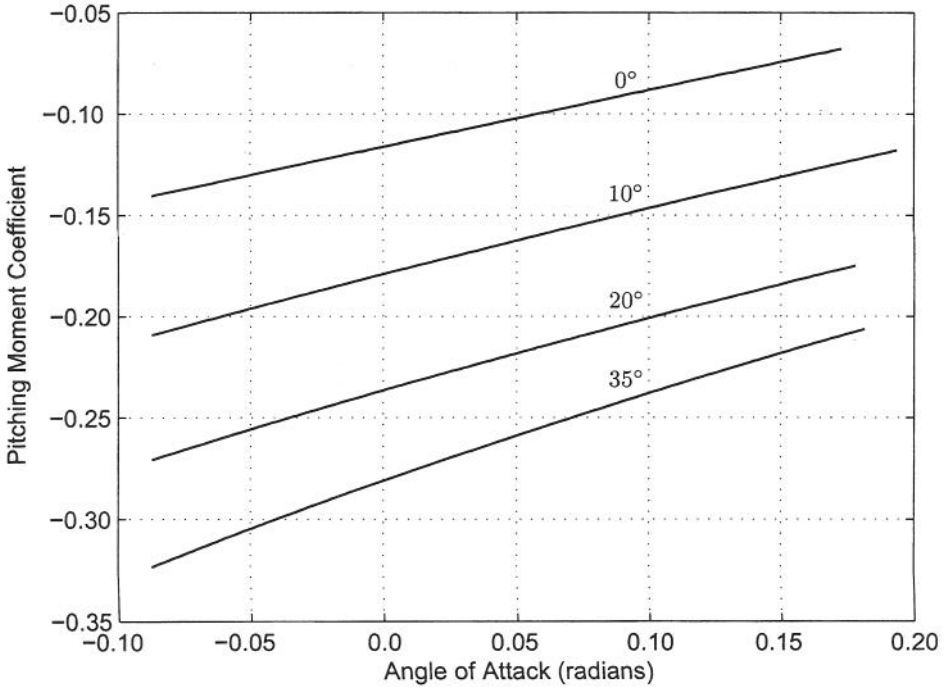


Figure 3.2: Variation of Pitching Moment Coefficient with Flap Setting

[1]The effect of aileron deflection on the pitching moment has been ignored.
[2]The pitching moment coefficients are about the body axes centre.

| Mach | $C_{M_{\alpha 0}}$ | $C_{M_0}$ | $(M_q)_b$ | $k_f$ | $\delta_f$ 10° $\Delta C_{M_{\alpha 0}}$ | 20° $\Delta C_{M_{\alpha 0}}$ | 35° $\Delta C_{M_{\alpha 0}}$ |
|---|---|---|---|---|---|---|---|
| 0.05 | -0.0772 | -0.0698 | -0.3689 | 0.7918 | -0.0629 | -0.1202 | -0.1655 |
| 0.10 | -0.0776 | -0.0701 | -0.3692 | 0.7961 | -0.0631 | -0.1206 | -0.1660 |
| 0.15 | -0.0781 | -0.0705 | -0.3697 | 0.7995 | -0.0634 | -0.1212 | -0.1668 |
| 0.20 | -0.0788 | -0.0711 | -0.3703 | 0.8027 | -0.0639 | -0.1221 | -0.1680 |
| 0.25 | -0.0798 | -0.0719 | -0.3712 | 0.8061 | -0.0645 | -0.1232 | -0.1696 |
| 0.30 | -0.0809 | -0.0729 | -0.3723 | 0.8101 | - | - | - |
| 0.35 | -0.0823 | -0.0742 | -0.3736 | 0.8146 | - | - | - |
| 0.40 | -0.0840 | -0.0758 | -0.3751 | 0.8197 | - | - | - |
| 0.45 | -0.0861 | -0.0777 | -0.3768 | 0.8255 | - | - | - |
| 0.50 | -0.0888 | -0.0800 | -0.3789 | 0.8323 | - | - | - |
| 0.55 | -0.0921 | -0.0827 | -0.3812 | 0.8402 | - | - | - |

Table 3.1: Variation of Pitching Moment Coefficients/Derivatives with Mach Number

| flap | | Mach 0.05 | 0.10 | 0.15 | 0.20 | 0.25 |
|---|---|---|---|---|---|---|
| 10° | $\alpha$ (rad) | | | $\Delta h_1$ | | |
| | 0.03491 | -0.00935 | -0.00887 | -0.00849 | -0.00818 | -0.00790 |
| | 0.06981 | -0.00930 | -0.00882 | -0.00844 | -0.00814 | -0.00786 |
| | 0.10472 | -0.01005 | -0.00954 | -0.00913 | -0.00881 | -0.00851 |
| | 0.13963 | -0.01104 | -0.01048 | -0.01004 | -0.00969 | -0.00937 |
| | 0.17453 | -0.01213 | -0.01153 | -0.01105 | -0.01067 | -0.01032 |
| | 0.20944 | -0.01328 | -0.01263 | -0.01211 | -0.01170 | -0.01132 |
| | 0.24435 | -0.01447 | -0.01376 | -0.01320 | -0.01276 | -0.01234 |
| 20° | $\alpha$ (rad) | | | $\Delta h_1$ | | |
| | 0.03491 | -0.02282 | -0.02172 | -0.02085 | -0.02016 | -0.01951 |
| | 0.06981 | -0.02003 | -0.01905 | -0.01827 | -0.01766 | -0.01708 |
| | 0.10472 | -0.01960 | -0.01864 | -0.01788 | -0.01728 | -0.01671 |
| | 0.13963 | -0.01993 | -0.01895 | -0.01818 | -0.01757 | -0.01700 |
| | 0.17453 | -0.02059 | -0.01959 | -0.01880 | -0.01817 | -0.01757 |
| | 0.20944 | -0.02145 | -0.02040 | -0.01958 | -0.01893 | -0.01831 |
| | 0.24435 | -0.02241 | -0.02133 | -0.02047 | -0.01979 | -0.01915 |
| 35° | $\alpha$ (rad) | | | $\Delta h_1$ | | |
| | 0.03491 | -0.05350 | -0.05106 | -0.04914 | -0.04762 | -0.04618 |
| | 0.06981 | -0.04421 | -0.04218 | -0.04058 | -0.03931 | -0.03811 |
| | 0.10472 | -0.04091 | -0.03903 | -0.03754 | -0.03637 | -0.03525 |
| | 0.13963 | -0.03956 | -0.03773 | -0.03629 | -0.03515 | -0.03408 |
| | 0.17453 | -0.03911 | -0.03730 | -0.03588 | -0.03475 | -0.03369 |
| | 0.20944 | -0.03916 | -0.03735 | -0.03593 | -0.03480 | -0.03373 |
| | 0.24435 | -0.03953 | -0.03770 | -0.03626 | -0.03513 | -0.03405 |

Table 3.2: Shift of Aero-Centre Position ($\Delta h_1$) with Mach Number and Flap Setting

# Chapter 4

# Sideforce Estimates

## 4.1 Wing-Body Contributions

The wing/body contribution to $Y_v$ was estimated, using the following formula from ESDU 79006, to be constant at -0.2627:

$$(Y_v)_{wb} = -\left[0.0174 + 0.674\frac{h^2}{S_b} + \frac{hbFF_w}{S_b}\left(4.95\frac{|z|}{h} - 0.12\right)\right]\frac{S_b}{S_W} - 0.0006|\Gamma|$$

The wing planform contribution to $Y_p$ was found, using ESDU 81014, to be dependent on lift coefficient as indicated below:

$$(Y_p)_w = (C_L)_{wb}\left[\frac{(Y_p)_w}{C_L}\right]$$

Where $(Y_p)_w/C_L$ is given in Table 4.1. The contribution to $Y_p$ arising from wing dihedral was

| Mach | $(Y_p)_w/C_L$ | $(a_{1i})_f$ rad$^{-1}$ | $(a_1)_f$ rad$^{-1}$ | $(Y_v)_f$ | $(a_1)_v$ rad$^{-1}$ | $(Y_v)_v$ | $Y_\zeta$ |
|---|---|---|---|---|---|---|---|
| 0.05 | 0.05000 | 2.920 | 2.710 | -0.698 | 1.335 | -0.0779 | 0.260 |
| 0.10 | 0.04995 | 2.925 | 2.739 | -0.706 | 1.336 | -0.0779 | 0.273 |
| 0.15 | 0.04988 | 2.932 | 2.759 | -0.711 | 1.338 | -0.0780 | 0.280 |
| 0.20 | 0.04980 | 2.942 | 2.776 | -0.715 | 1.340 | -0.0782 | 0.284 |
| 0.25 | 0.04970 | 2.956 | 2.793 | -0.720 | 1.343 | -0.0783 | 0.288 |
| 0.30 | 0.04956 | 2.973 | 2.812 | -0.725 | 1.346 | -0.0785 | 0.291 |
| 0.35 | 0.04940 | 2.994 | 2.834 | -0.730 | 1.351 | -0.0788 | 0.294 |
| 0.40 | 0.04918 | 3.018 | 2.857 | -0.736 | 1.356 | -0.0791 | 0.297 |
| 0.45 | 0.04890 | 3.047 | 2.882 | -0.743 | 1.362 | -0.0794 | 0.300 |
| 0.50 | 0.04860 | 3.080 | 2.911 | -0.750 | 1.369 | -0.0798 | 0.303 |
| 0.55 | 0.04825 | 3.119 | 2.944 | -0.759 | 1.378 | -0.0804 | 0.307 |

Table 4.1: Variation of Sideforce Derivatives with Mach Number

estimated using the following formula from ESDU 85006:

$$\frac{(Y_p)_\Gamma}{(L_p)_w} = \frac{4\sin\Gamma}{1+3\lambda}\left[1 + 2\lambda - 3\frac{z}{s}(1+\lambda)\sin\Gamma\right] = 0.3924$$

The contribution to $Y_r$ from the fuselage is given by the following expression from ESDU 83026

$$(Y_r)_b = -0.04\frac{l_b S_b}{bS_W}$$

As $l_b$ = 13.347 m and $S_b$ = 21.076 m$^2$,then $(Y_r)_b$ = -0.0283.

## 4.2 Engine Nacelle Contributions

The contribution to $Y_v$ arising from the engine nacelles was determined using the following formula from ESDU 00025 and found to be constant at -0.0458:

$$(Y_v)_n = -\frac{2}{3}\frac{K\pi h_n^2}{S_W}$$

## 4.3 Fin Contributions

The fin contribution to $Y_v$ was estimated using the following formula from ESDU 82010 and is based on the lift curve slope, $(a_1)_f$, obtained from ESDU 70011 assuming a trapezoidal fin shape, see Table 4.1. Viscous effects were estimated using ESDU 97020 in a similar manner to that applied to the tailplane, see Appendix B.

$$(Y_v)_f = -J_B J_T J_W (a_1)_f \frac{S_F}{S_W}$$

Given that $J_B = 1.10$, $J_T = 0.985$ and $J_W = 1.26$ then $(Y_v)_f$ is as given in Table 4.1. The ventral fin contribution to $Y_v$ was determined from ESDU 92029 using the following formula:

$$(Y_v)_v = -(a_1)_v K_v \frac{S_v}{S_W}$$

The lift curve slope $(a_1)_v$ was found using ?, see Table 4.1. Given that $K_v = 4.31$ and $S_v = 0.339$ m$^2$ then $(Y_v)_v$ is as given Table 4.1. The fin contribution to $Y_p$ was found, using ESDU 83006, to be a function of body incidence, $\alpha$, and sidewash, which was itself dependent on incidence. Thus:

$$(Y_p)_f = -1.377\,(0.060\cos\alpha - 0.444\sin\alpha - 0.18 - \sigma_\alpha)$$

Where $\sigma_\alpha$ is obtained from Table 4.2.

| $0.060(1-\cos\alpha)+0.444\sin\alpha$ | 0.00 | 0.05 | 0.10 | 0.15 | 0.20 | 0.25 |
|---|---|---|---|---|---|---|
| $\sigma_\alpha$ | 0.00 | 0.07 | 0.15 | 0.25 | 0.35 | 0.45 |

Table 4.2: Variation of Sidewash Factor with Body Incidence

The fin contribution to $Y_r$ was estimated using the following formula from ESDU 82017:

$$(Y_r)_f = J_B J_T \frac{(a_1)_f}{b}\frac{S_F}{S_W}\left[(z_{crF} + 0.85\bar{z}_F)\sin\alpha + (m_F + 0.7\bar{z}_F\tan\Lambda_{0.25F})\cos\alpha\right]$$

As $\bar{z}_F = 1.133$ m, $z_{crF} = 0.608$ m and $m_F = 5.607$ m, then:

$$(Y_r)_f = \frac{-(Y_v)_f}{J_W b}\left[1.571\sin\alpha + 6.339\cos\alpha\right]$$

## 4.4 Rudder Contributions

The rudder sideforce derivative[1], $Y_\zeta$, was determined using ESDU 87008 along with some of the data obtained in the estimation of $(Y_v)_f$. So:

$$Y_\zeta = J_R J_T (a_1)_f \frac{S_F}{S_W}\alpha_\delta \Delta\Phi$$

Given that $J_R = 0.769$, $J_T = 0.985$ and $\Delta\Phi = 1.0$ then $Y_\zeta$ is as given in Table 4.1

[1]The rudder deflection is measured in a plane parallel to the body axis

## 4.5 Flap Contributions

The flap contribution to $Y_v$ was estimated using the following equation obtained from ESDU 81013:

$$(Y_v)_{flap} = -\Delta C'_{D_f} + \left[0.045\,(Y_v)_f + 0.003\right] \Delta C_{L_f}$$

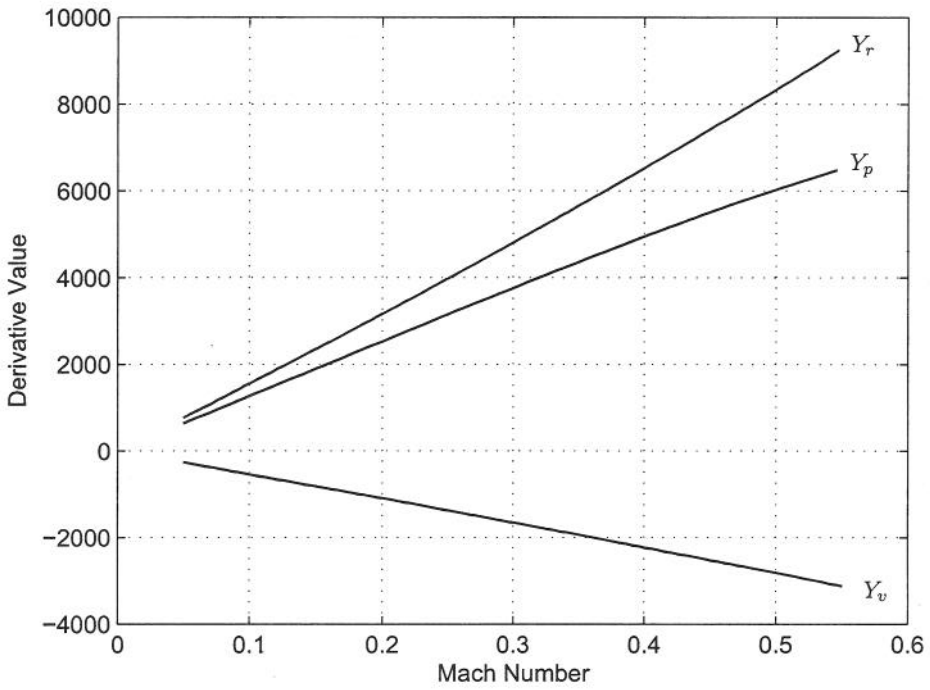


Figure 4.1: Variation of Sideforce Derivatives (constant incidence, no flap)

# Chapter 5

# Rolling Moment Estimates

## 5.1 Wing-Body Contributions

The contribution to $L_v$ arising from wing dihedral was determined using ESDU Aero A.06.01.03 and found to be dependent on Mach number as shown in Table 5.1 as was the case for the wing planform contribution to $L_p$ obtained from ESDU Aero A.06.01.01.

| Mach | $(L_v)_\Gamma$ | $(L_v)_w/C_L$ | $(L_p)_w$ | $L_r/L_{r0}$ |
|---|---|---|---|---|
| 0.05 | -0.1058 | 0.0263 | -0.2572 | 1.005 |
| 0.10 | -0.1068 | 0.0263 | -0.2593 | 1.010 |
| 0.15 | -0.1077 | 0.0263 | -0.2610 | 1.015 |
| 0.20 | -0.1087 | 0.0263 | -0.2628 | 1.020 |
| 0.25 | -0.1097 | 0.0263 | -0.2648 | 1.030 |
| 0.30 | -0.1109 | 0.0263 | -0.2671 | 1.045 |
| 0.35 | -0.1122 | 0.0263 | -0.2700 | 1.060 |
| 0.40 | -0.1140 | 0.0263 | -0.2740 | 1.080 |
| 0.45 | -0.1161 | 0.0270 | -0.2790 | 1.105 |
| 0.50 | -0.1190 | 0.0284 | -0.2857 | 1.135 |
| 0.55 | -0.1219 | 0.0303 | -0.2935 | 1.170 |

Table 5.1: Variation of Rolling Moment Derivatives with Mach Number

The wing planform contribution to $L_v$ was estimated from ESDU 80033 and is expressed in the form $(L_v)_w/C_L$, see Table 5.1. As the effect of flaps is covered separately only the basic wing lift coefficient is required here. Using ESDU 73006, the fuselage contribution to $L_v$ was found to be given by:

$$(L_v)_b = -0.014\frac{l_b}{l}\frac{S_b}{S_w}\alpha_b = -0.00145\alpha_b$$

where $\alpha_b$ is measured in degrees. Similarly, the contribution arising from wing-body interference was estimated to be equal to a constant value of 0.0445. The dihedral contribution to $L_p$ was determined using the following formula from ESDU 85006:

$$\frac{(L_p)_\Gamma}{(L_p)_w} = \frac{-2\sin\Gamma}{1+3\lambda}\left[2+4\lambda-3\frac{z}{s}(1+\lambda)\sin\Gamma\right]\frac{z}{s} = -0.0466$$

The wing contribution to $L_r$ was determined from ESDU 72021 and is given by the following formula for incompressible flow. Account was made of compressibility effects by using a scaling

factor, also obtained from ESDU 72021, see Table 5.1

$$(L_{r0})_w = 0.109C_L - 0.0037$$

## 5.2 Nacelle Contributions

The contribution to $L_v$ arising from the engine nacelles was determined using the following formula from ESDU 00025:

$$(L_v)_n = -\frac{z_0}{b}(Y_v)_n + 0.86\,[(L_v)_n]_T$$

Given that $[(L_v)_n]_T$ = 0.0181 and $(Y_v)_n$= -0.0458 then $(L_v)_n$ = 0.0165. This aeronormalised derivative is invariant with Mach number and incidence.

## 5.3 Aileron Contributions

The rolling moment due to aileron deflection, $L_\xi$, was determined using ESDU 88013 and was based on an estimate of lift curve slope, $a_2$, obtained from ESDU 74011. Thus for each aileron[1]:

$$L_\xi = -\frac{1}{4}(\eta_i + \eta_o)(a_2)_a(\Phi_i - \Phi_0)\cos\Lambda_H$$

Given that $\eta_i$ = 0.602, $\eta_o$ = 0.975 and $\Lambda_H$ = 5.4° and noting that the function quoted in ESDU 88013 is based on inviscid estimates of $(a_1)_w$, $L_\xi$ is as given in Table 5.2:

| Mach | $(a_2)_a$ | $\Phi_i$ | $\Phi_0$ | $L_\xi$ |
|---|---|---|---|---|
| 0.05 | 3.3351 | 0.2645 | 0.0105 | -0.3325 |
| 0.10 | 3.5210 | 0.2630 | 0.0105 | -0.3490 |
| 0.15 | 3.6159 | 0.2620 | 0.0105 | -0.3570 |
| 0.20 | 3.7126 | 0.2610 | 0.0105 | -0.3650 |
| 0.25 | 3.7834 | 0.2595 | 0.0105 | -0.3698 |
| 0.30 | 3.8682 | 0.2570 | 0.0105 | -0.3743 |
| 0.35 | 3.9723 | 0.2545 | 0.0105 | -0.3804 |
| 0.40 | 4.0842 | 0.2520 | 0.0105 | -0.3872 |
| 0.45 | 4.2231 | 0.2495 | 0.0105 | -0.3962 |
| 0.50 | 4.4035 | 0.2445 | 0.0105 | -0.4045 |
| 0.55 | 4.6483 | 0.2370 | 0.0105 | -0.4133 |

Table 5.2: Variation of Aileron Rolling Moment Derivative with Mach Number

## 5.4 Fin Contributions

The fin contribution to $L_v$ was estimated from the following formula given in ESDU 82010:

$$(L_v)_f = \frac{(Y_v)_f}{b}\left[(z_{crF} + 0.85\bar{z}_F)\cos\alpha - (m_F + 0.7\bar{z}_F\tan\Lambda_{0.25F})\sin\alpha\right]$$

As $\bar{z}_F$ = 1.133 m, $z_{crF}$ = 0.608 m and $m_F$ = 5.607 m, then:

$$(L_v)_f = \frac{(Y_v)_f}{b}\left[1.571\cos\alpha - 6.339\sin\alpha\right]$$

[1]Positive surface deflection is starboard down and port up

Using an analogous method the ventral fin contribution to $L_v$ is given by:

$$(L_v)_v = \frac{(Y_v)_v}{b}\left[z_v \cos\alpha - m_v \sin\alpha\right] = -\frac{(Y_v)_v}{b}\left[0.524\cos\alpha + 6.335\sin\alpha\right]$$

Similarly the fin contribution to $L_p$ is given, from ESDU 83006, by:

$$(L_p)_f = -\frac{(Y_p)_f}{b}\left[0.946\cos\alpha - 7.042\sin\alpha\right]$$

Likewise, from ESDU 82017, the fin contribution to $L_r$ is given by

$$(L_r)_f = \frac{(Y_r)_f}{b}\left[1.571\cos\alpha - 6.339\sin\alpha\right]$$

## 5.5 Rudder Contributions

The rudder rolling moment derivative, $L_\zeta$, was determined using the following formula from ESDU 87008:

$$L_\zeta = \frac{Y_\zeta}{b}\left[z_R \cos\alpha - l_R \sin\alpha\right]$$

Given that:

$$z_R = h_{Ri} + 0.5h_R = 0.363 + 0.4 \times 2.837$$
$$l_R = (m_F + 0.7\bar{z}_F \tan\Lambda_{0.25F}) + 0.25c_F = 6.339 + 0.25 \times 1.975$$

Then:

$$L_\zeta = \frac{Y_\zeta}{b}\left[1.498\cos\alpha - 6.833\sin\alpha\right]$$

## 5.6 Flaps

The contribution to $L_v$ arising from flap deployment was determined using the following formula from ESDU 80034:

$$(L_v)_f = 0.0322\Delta C_{L_f}$$

The flap contribution to $L_r$ for incompressible flow was determined from ESDU 72021, using section lift coefficient increment values obtained from ESDU 93019, see Table 5.3. Account was made of compressibility effects by using a scaling factor, also estimated from ESDU 72021, see Table 5.1

| $\delta_f$ | 10° | 20° | 35° |
|---|---|---|---|
| $(L_{r0})_f$ | -0.0096 | -0.0180 | -0.0245 |

Table 5.3: Flap Contribution to Rolling Moments

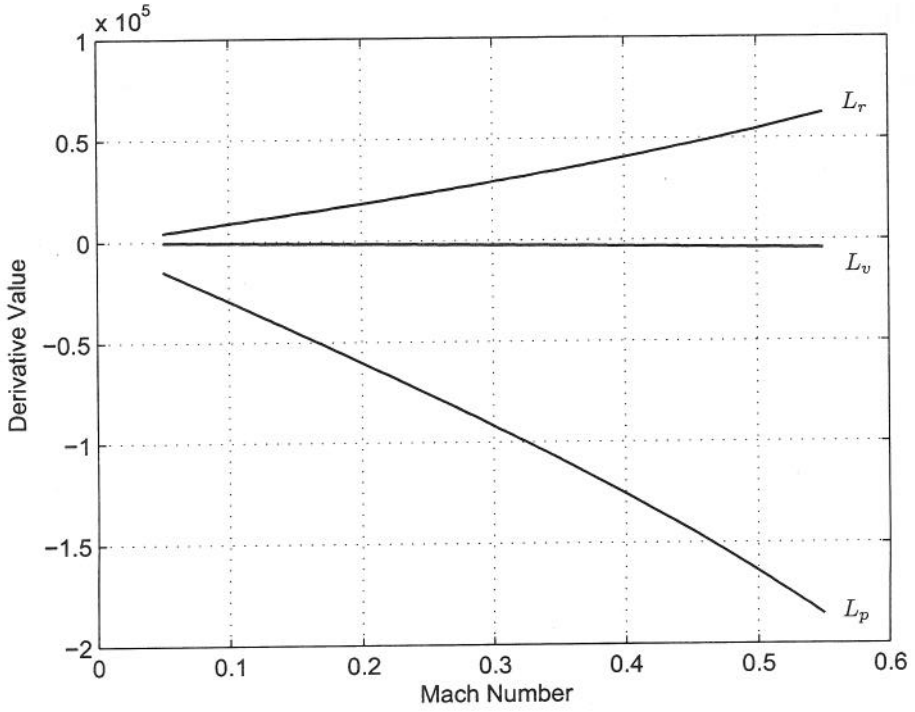


Figure 5.1: Variation of Rolling Moment Derivatives (constant incidence, no flap)

# Chapter 6

# Yawing Moment Estimates

## 6.1 Wing-Body Contributions

The wing/body contribution to $N_v$ was estimated using ESDU 79006, thus:

$$(N_v)_{wb} = (N_v)_{mid} + \frac{l - 0.5l_b}{b}(Y_v)_{wb} = -0.086\left[\frac{S_b l_b}{S_W b}\right] + \frac{l - 0.5l_b}{b}(Y_v)_{wb}$$

As $(Y_v)_{wb}$ = -0.2627 then $(N_v)_{wb}$ = -0.0719. This aeronormalised derivative is invariant with Mach number and incidence. The wing planform contribution to $N_p$ was found, using ESDU 81014, to be dependent on lift coefficient as indicated below:

$$\begin{aligned}
(N_p)_w &= (C_L)_{wb}\left[\frac{(N_p)_w}{C_L}\right] + \frac{(N_p)_w}{(dC'_D/d\alpha)}\frac{dC'_D}{d\alpha} \\
&= (C_L)_{wb}\left[\frac{(N_p)_w}{C_L}\right] + 0.0244\frac{dC'_D}{dC_L}\frac{dC_L}{d\alpha} \\
&= (C_L)_{wb}\left[\frac{(N_p)_w}{C_L}\right] + 0.0244 \times 0.00154\,(C_L)_{wb}\frac{dC_L}{d\alpha} \\
(N_p)_w &= (C_L)_{wb}\left[\frac{(N_p)_w}{C_L} + 0.000038\,(a_1)_{wb}\right]
\end{aligned}$$

Where $(N_p)_w/C_L$ is given in Table 6.1 and $(a_1)_{wb}$ is given in Table 1.5.

| Mach | $(N_p)_w/C_L$ | $G(\eta_i)$ | $G(\eta_o)$ |
|---|---|---|---|
| 0.05 | -0.03896 | 0.0600 | 0.1000 |
| 0.10 | -0.03890 | 0.0635 | 0.1035 |
| 0.15 | -0.03884 | 0.0670 | 0.1070 |
| 0.20 | -0.03873 | 0.0705 | 0.1105 |
| 0.25 | -0.03861 | 0.0740 | 0.1140 |
| 0.30 | -0.03842 | 0.0775 | 0.1175 |
| 0.35 | -0.03822 | 0.0810 | 0.1210 |
| 0.40 | -0.03799 | 0.0845 | 0.1245 |
| 0.45 | -0.03765 | 0.0880 | 0.1280 |
| 0.50 | -0.03725 | 0.0915 | 0.1315 |
| 0.55 | -0.03686 | 0.0950 | 0.1350 |

Table 6.1: Variation of Yawing Moment Derivative Factors with Mach Number

The contribution to $N_p$ arising from wing dihedral was determined using the following formula from ESDU 85006:

$$\frac{(N_p)_\Gamma}{(L_p)_w} = \frac{-\sin\Gamma}{3(1+3\lambda)(1+\lambda)}\left[6\frac{x}{s}(1+\lambda)\left\{1+2\lambda-3\frac{z}{s}(1+\lambda)\sin\Gamma\right\}+\left(1+4\lambda+\lambda^2\right)\tan\Lambda_{0.25}\right]$$
$$= 0.0019$$

The wing contribution to $N_r$ was estimated using the following formula from ESDU 71017:

$$(N_r)_w = -0.1238\left[(C_{D0})_w + 0.305\Delta C_{D0_f}\right] - 0.0053\,(C_L)^2_{wb}$$

The contribution to $N_r$ from the fuselage is given by the following expression from ESDU 83026

$$(N_r)_b = -0.01\frac{l_b^2 S_b}{b^2 S_W}$$

As $l_b$ = 13.347 m and $S_b$ = 21.076 m$^2$,then $(N_r)_b$ = -0.0060.

## 6.2 Nacelle Contributions

The contribution to $N_v$ arising from the engine nacelles was determined using the following formula from ESDU 00025:

$$(N_v)_n = (Y_v)_n\frac{m_0 - 0.46l_n}{b}$$

As $(Y_v)_n$ = -0.0458 then $(N_v)_n$ = -0.0005. This aeronormalised derivative is also invariant with Mach number and incidence.

## 6.3 Aileron Contributions

The yaw moment arising from aileron deflection, $\mathcal{N}_\xi$ is caused by antisymmetric changes in wing drag, now from ESDU 88029:

$$\mathcal{N}_\xi = \bar{q}Sb\left(C_{n_i} + C_{n_p}\right) = \bar{q}Sb\left(F\left(\eta_i\right) - F\left(\eta_o\right) + C_{n_p}\right)$$

where, using the average aileron deflection, $\xi$:

$$F(\eta) = \left[\frac{H(\eta)}{A}\left(0.498\left[\xi_p - \xi_s\right] + 2.8 + 18\Delta C_{L_f}\right) - G(\eta)\,(C_L)_w\right]L_{\xi}.\xi$$

and:

$$C_{n_p} = 0.0119\Bigg\{\left[1-0.0665\left(1-\frac{|\xi_s|}{\xi_s}\right)\right](0.0897+\xi_s)^2$$
$$-\left[1-0.0665\left(1+\frac{|\xi_p|}{\xi_p}\right)\right](0.0897-\xi_p)^2\Bigg\}$$

Note that $H(\eta_i)$ = 0.0770 and $H(\eta_o)$ = 0.0715. See Table 6.1 for $G(\eta)$.

## 6.4 Fin Contributions

The fin contribution to $N_v$ was estimated from the following formula given in ESDU 82010:

$$(N_v)_f = -\frac{(Y_v)_f}{b}\left[(z_{crF} + 0.85\bar{z}_F)\sin\alpha + (m_F + 0.7\bar{z}_F \tan\Lambda_{0.25F})\cos\alpha\right]$$

As $\bar{z}_F = 1.133$ m, $z_{crF} = 0.608$ m and $m_F = 5.607$ m, then:

$$(N_v)_f = -\frac{(Y_v)_f}{b}\left[1.571\sin\alpha + 6.339\cos\alpha\right]$$

Using an analogous method the ventral fin contribution to $N_v$ is given by:

$$(N_v)_v = -\frac{(Y_v)_v}{b}\left[z_v\sin\alpha + m_v\cos\alpha\right] = -\frac{(Y_v)_v}{b}\left[6.335\cos\alpha - 0.524\sin\alpha\right]$$

Similarly the fin contribution to $N_p$ is given, from ESDU 83006, by:

$$(N_p)_f = -\frac{(Y_p)_f}{b}\left[0.946\sin\alpha + 7.042\cos\alpha\right]$$

Likewise, from ESDU 82017, the fin contribution to $N_r$ is given by

$$(N_r)_f = -\frac{(Y_r)_f}{b}\left[1.571\sin\alpha + 6.339\cos\alpha\right]$$

## 6.5 Rudder Contributions

The rudder yawing moment derivative, $N_\zeta$, was determined using the following formula from ESDU 87008:

$$N_\zeta = -\frac{Y_\zeta}{b}\left[l_R\cos\alpha + z_R\sin\alpha\right] = -\frac{Y_\zeta}{b}\left[6.833\cos\alpha + 1.498\sin\alpha\right]$$

## 6.6 Flap Contribution

The flap contribution to $N_v$ was estimated using the following equation obtained from ESDU 81013:

$$(N_v)_{flap} = 0.196\Delta C'_{D_f} + 0.045\,(N_v)_f\,\Delta C_{L_f}$$

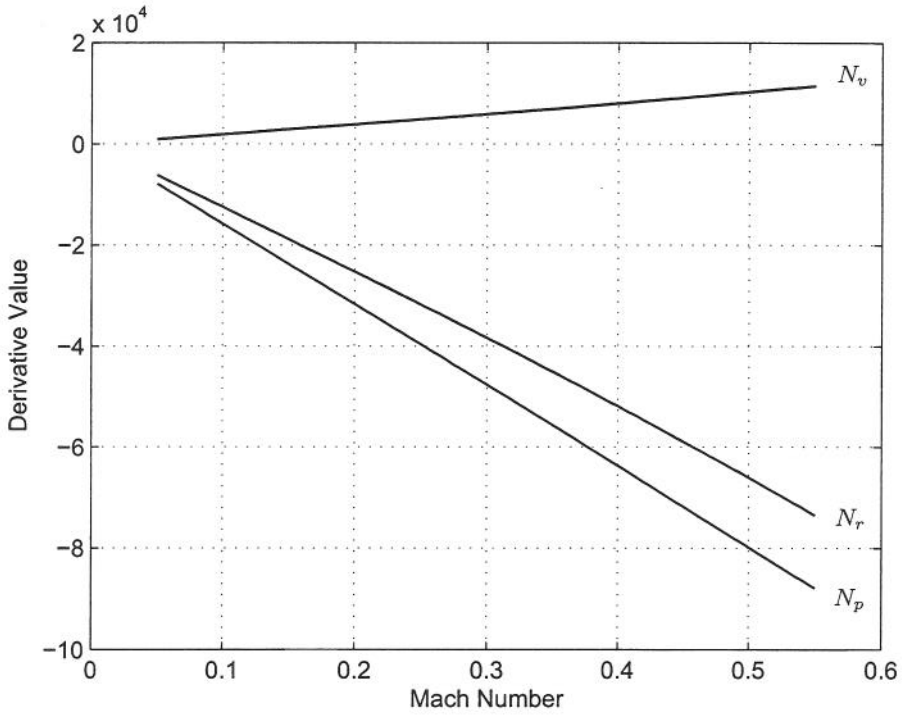


Figure 6.1: Variation of Yawing Moment Derivatives (constant incidence, no flap)

# Chapter 7

# Body Axes Referenced Derivatives

The lateral and directional derivative estimates given earlier are all wind axes referenced and therefore need to be converted to a body axes reference. From Cook [1997]

$$
\begin{aligned}
Y_{v_b} &= Y_{v_w} \\
Y_{\zeta_b} &= Y_{\zeta_w} \\
Y_{p_b} &= Y_{p_w}\cos\alpha - Y_{r_w}\sin\alpha \\
Y_{r_b} &= Y_{r_w}\cos\alpha + Y_{p_w}\sin\alpha \\
L_{v_b} &= L_{v_w}\cos\alpha - N_{v_w}\sin\alpha \\
N_{v_b} &= N_{v_w}\cos\alpha + L_{v_w}\sin\alpha \\
L_{\zeta_b} &= L_{\zeta_w}\cos\alpha - N_{\zeta_w}\sin\alpha \\
N_{\zeta_b} &= N_{\zeta_w}\cos\alpha + L_{\zeta_w}\sin\alpha \\
L_{\xi_b} &= L_{\xi_w}\cos\alpha - N_{\xi_w}\sin\alpha \\
N_{\xi_b} &= N_{\xi_w}\cos\alpha + L_{\xi_w}\sin\alpha \\
L_{p_b} &= L_{p_w}\cos^2\alpha + N_{r_w}\sin^2\alpha - (L_{r_w} + N_{p_w})\sin\alpha\cos\alpha \\
N_{p_b} &= N_{p_w}\cos^2\alpha - L_{r_w}\sin^2\alpha + (L_{p_w} - N_{r_w})\sin\alpha\cos\alpha \\
L_{r_b} &= L_{r_w}\cos^2\alpha - N_{p_w}\sin^2\alpha - (L_{p_w} - N_{r_w})\sin\alpha\cos\alpha \\
N_{r_b} &= N_{r_w}\cos^2\alpha + L_{p_w}\sin^2\alpha + (L_{r_w} + N_{p_w})\sin\alpha\cos\alpha
\end{aligned}
$$

# References


ESDU 00025. *Computer program for the prediction of aircraft lateral stability derivatives in sidelsip at subsonic speeds.* September 2000.

ESDU 01007. *Trailing vortex drag factors for wings with part-span trailing-edge plain flaps.* ESDU International. November 2001.

ESDU Wings 01.01.04. *Effect of cut-out on lift-curve slope.* ESDU International. With Amendment A, May 1974.

ESDU Flaps 02.01.07. *Conversion factor for profile drag increment for part-span flaps.* ESDU International. With Amendments A to C, February 1993.

ESDU Wings 02.04.02. *Profile drag of smooth wings.* ESDU International. July 1947.

ESDU 03017. *Pitching moment curve of wings with leading-edge and trailing-edge high-lift devices deployed at low speed.* ESDU International. September 2003.

ESDU Aircraft 06.01.01. *Stability derivative L sub p , rolling moment due to rolling for swept and tapered wings.* ESDU International. With Amendment A, March 1981.

ESDU Aircraft 06.01.03. *Stability derivative (L sub v) sub Gamma. Contrbution of full-span dihedral to rolling moment due to sideslip.* ESDU International. With Amendments A and B, April 1973.

ESDU Controls 08.01.01. *rate of change of pitching moment coefficient with control deflection for a plain control in incompressible two-dimensional flow, m sub zero.* ESDU International. With Amendment A, March 1981.

ESDU 66032. *Subsonic lift-dependent drag due to boundary layer of plane, symmetrical section wings.* ESDU International. With Amendments A to E, November 2002.

ESDU 70011. *Lift-curve slope and aerodynamic centre position of wings in inviscid subsonic flow.* ESDU International. With Amendments A to I, August 1996.

ESDU 71017. *Aero-normalised stability derivatives: effect of wing on yawing moment due to yawing.* ESDU International. September 1971.

ESDU 72021. *Effect of wing on rolling moment due to yawing.* ESDU International. Reprinted with Amendments A and B, June 1986.

ESDU 72024. *Aerodynamic characteristics of aerofoils in compressible inviscid airflow at sub-critical Mach numbers.* ESDU International. Reprinted with Amendments A to D, January 1999.

ESDU 73006. *Effects of isolated body and wing-body interference on rolling moment due to sideslip: L sub v (with Addendum A for nacelle effects).* ESDU International. Reprinted with Amendments A to C, March 1999.

ESDU 74011. *Rate of change of lift coefficient with control deflection for full-span plain controls.* ESDU International. With Amendment A, March 1997.

ESDU 74035. *Subsonic lift-dependent drag due to the trailing vortex wake for wings without camber or twist.* ESDU International. With Amendment A, April 1996.

ESDU 77021. *Properties of a standard atmosphere.* ESDU International. With Amendment A, June 1986.

ESDU 77028. *Geometrical characteristics of typical bodies.* ESDU International. With Amendments A to F, July 1990.

ESDU 78019. *Profile drag of axisymmetric bodies at zero-incidence for subcritical Mach numbers.* ESDU International. With Amendments A and B, July 1998.

ESDU 79006. *Wing-body yawing moment and sideforce derivatives due to sideslip: Nv and Yv (with Addendum A for nacelle effects).* ESDU International. Reprinted with amendments A and B, March 1999.

ESDU 80020. *Average downwash at the tailplane at low angles of attack and subsonic speeds.* ESDU International. With Amendments A , October 1981.

ESDU 80033. *Contridution of wing planform to rolling moment derivative due to sideslip, (L sub V) sub w, at subsonic speeds.* ESDU International. With Amendment A, October 1981.

ESDU 80034. *Effect of trailing-edge flaps on rolling moment derivative due to sideslip, (L sub v) sub f.* ESDU International. November 1980.

ESDU 81013. *Effect of trailing edge flaps on sidefocre and yawing moment derivatives due to sideslip, (Y sub v) sub f and (N sub v) sub f.* ESDU International. With Amendment A, June 1982.

ESDU 81014. *Contribution of wing planform to derivatives of yawing moment and sideforce due to roll rate at subsonic speeds, (N sub p) sub w and (Y sub p) sub w.* ESDU International. June 1981.

ESDU 82010. *Contribution of fin to sideforce, yawing moment and rolling moment derivatives due to sideslip, (Y sub v) sub F, (N sub v) sub F, (L sub v) sub F, in the presence of body, wing and tailplane.* ESDU International. With Amendments A to C, April 1993.

ESDU 82017. *Contribution of fin to sideforce, yawing moment and rolling moment derivatives due to yaw rate, (Y sub v) sub F, (N sub v) sub F, (L sub v) sub F.* ESDU International. Issued July 1983.

ESDU 83006. *Contribution of fin to sideforce, yawing moment and rolling moment derivatives due to rate of roll, (Y sub p) sub F, (N sub p) sub F, (L sub P) sub F, in the presence of body, wing and tailplane.* ESDU International. With Amendment A, March 1985.

ESDU 83026. *Contribution of body to yawing moment and sideforce derivatives due to rate of yaw, (N sub r) sub B and (Y sub r) sub B.* ESDU International. August 1983.

ESDU 83040. *Method for the rapid estimation of spanwise loading of wings with camber and twist in subsonic attached flow.* ESDU International. With Amendments A to C, July 1985.

ESDU 84026. *Aerofoil maximum lift coefficient for Mach numbers up to 0.4.* ESDU International. Reprinted with Amendments A to C, January 1999.

ESDU 85006. *Contibution of wing dihedral to sideforce, yawing moment and rolling moment derivatives due to rate of roll at subsonic speeds, (Y sub p) sub Gamma, (N sub p) sub Gamma and (L sub p) sub Gamma.* ESDU International. March 1985.

ESDU 87001. *Wing pitching moment at zero lift at subcritical Mach numbers.* ESDU International. With Amendments A and B, August 1991.

ESDU 87005. *Increment in aerofoil profile drag coefficient due to the deployment of a single-slotted flap.* ESDU International. With Amendments A to C, March 1999.

ESDU 87008. *Rudder sideforce, yawing moment and rolling moment control derivatives at low speed: Y sub zeta, N sub zeta and L sub zeta.* ESDU International. With Amendments A to G, January 1994.

ESDU 87024. *Low-speed drag coefficient increment at constant lift due to full-span plain flaps.* ESDU International. With Amendments A to C, March 2000.

ESDU 87031. *Wing angle of attack for zero lift at subcritical Mach numbers.* ESDU International. Reprinted with Amendment A, January 1999.

ESDU 88013. *Rolling moment derivative, L sub xi, for ailerons at subsonic speeds.* ESDU International. With Amendments A and B, October 1992.

ESDU 88029. *Yawing moment coefficient for plain ailerons at subsonic speeds.* ESDU International. With Amendments A and B, October 1992.

ESDU 89029. *Installed tailplane lift-curve slope at subsonic speeds.* ESDU International. October 1989.

ESDU 89034. *The maximum lift coefficient of plain wings at subsonic speeds.* ESDU International. With Amendment A, August 1993.

ESDU 89042. *Body effect on wing angle of attack and pitching moment at zero lift at low speeds.* ESDU International. November 1989.

ESDU 90010. *Pitching moment and lift force derivatives due to rate of pitch for aircraft at subsonic speeds.* ESDU International. With Amendments A, November 1990.

ESDU 91007. *Lift-curve slope of wing-body combinations.* ESDU International. With Amendments A to D, December 1995.

ESDU 91014. *Maximum lift of wings with trailing-edge flaps at low speeds.* ESDU International. With Amendment A, August 1995.

ESDU 92029. *Contribution of ventral fins to sideforce and yawing moment derivatives due to sideslip at low angle of attack.* ESDU International. With Amendments A and B, October 1993.

ESDU 93019. *Wing lift coefficient at zero angle of attack due to deployment of single-slotted flaps at low speeds.* ESDU International. With Amendment A, July 1995.

ESDU 96003. *Lift curve of wings with high-lift devices deployed at low speed.* ESDU International. 96003, reprinted with Amendments A to E, November 2003.

ESDU 97002. *Information on the use of Data Items on high-lift devices.* ESDU International. With Amendment A, November 2003.

ESDU 97003. *Fuselage interference effects on flap characteristics.* ESDU International. March 1997.

ESDU 97020. *Slope of aerofoil lift curve slope for subsonic two-dimensional flow.* ESDU International. September 1997.

ESDU 97021. *Effect of trailing-edge flap deployment on average downwash at the tailplane at low speeds.* ESDU International. September 1997.

ESDU 98011. *Aerofoil incidence for zero lift in subsonic two-dimensional flow.* ESDU International. September 1998.

ESDU 98017. *Aerofoil and wing pitching moment coefficient at zero angle of attack due to the deployment of trailing-edge plain flaps at low speeds.* ESDU International. With Amendment A, November 2003.

ESDU 99004. *Aerofoil and wing pitching moment coefficient at zero angle of attack due to deployment of trailing-edge single-slotted flaps at low speed.* ESDU International. With Amendments A and B, November 2002.

M. Cook. *Flight Dynamics Principles.* Arnold, London, 1997.

S Intarajaiour. A study of the lateral stability and control characteristics of the Jetstream aircraft G-AUXI. Master's thesis, College of Aeronautics, Cranfield Institute of Technology, September 1983.

B. McCormick. *Aerodynamics, Aeronautics and Flight Mechanics.* John Wiley & Sons, Inc., New York, 1979.

# Appendix A

# Aircraft Particulars

## A.1 Geometric Details

### A.1.1 Wing

| | | | | |
|---|---|---|---|---|
| span | 52.0 | ft | 15.85 | m |
| gross area | 270.0 | $ft^2$ | 25.08 | $m^2$ |
| exposed area | 225.4 | $ft^2$ | 20.94 | $m^2$ |
| aerodynamic mean chord | 6.1 | ft | 1.86 | m |
| root chord (3 ft from centreline) | 7.2 | ft | 2.19 | m |
| root datum chord (on centreline) | 7.8 | ft | 2.38 | m |
| aspect ratio | 10.0 | | | |
| taper ratio - tip/centreline | 0.333 | | | |
| sweep of 30% chordline | 0.0° | | | |
| root aerofoil section | NACA 63A418 | | | |
| tip aerofoil section | NACA 63A412 | | | |
| twist | -2° | washout | | |

Additional dimensions scaled from Intarajaiour [1983].

### A.1.2 Fuselage

| | | | | |
|---|---|---|---|---|
| maximum diameter | 6.5 | ft | 1.981 | m |
| length | 43.79 | ft | 13.347 | m |
| plan area | 226.8 | $ft^2$ | 21.076 | $m^2$ |
| side area | 226.8 | $ft^2$ | 21.076 | $m^2$ |

### A.1.3 Tailplane

| | | | | |
|---|---|---|---|---|
| span | 21.67 | ft | 6.604 | m |
| gross area | 83.8 | $ft^2$ | 7.785 | $m^2$ |
| aerodynamic mean chord | 4.10 | ft | 1.250 | m |
| root chord | 5.50 | ft | 1.676 | m |
| aspect ratio | 5.6 | | | |
| taper ratio - tip/centreline | 0.409 | | | |
| root aerofoil section | NACA 0012 | | | |
| tip aerofoil section | NACA 0010 | | | |
| quarter chord sweep | 7.1° | | | |

### A.1.4 Fin

| | | | |
|---|---|---|---|
| area | 50.96 | ft$^2$ | 4.734 m$^2$ |
| tip chord | 2.92 | ft | 0.889 m |
| root chord | 9.07 | ft | 2.764 m |
| height | 8.50 | ft | 2.592 m |
| aspect ratio | 2.838 | | |
| taper ratio | 0.322 | | |
| root aerofoil section | NACA 0012 | | |
| tip aerofoil section | NACA 0010 | | |
| quarter chord sweep | 42.7° | | |

The root chord and height are measured from the intersection of the quarter chord sweep line with fuselage.

### A.1.5 Engine

| | | | | |
|---|---|---|---|---|
| length | 9.426 | ft | 2.873 | m |
| offset | 8.848 | ft | 2.697 | m |

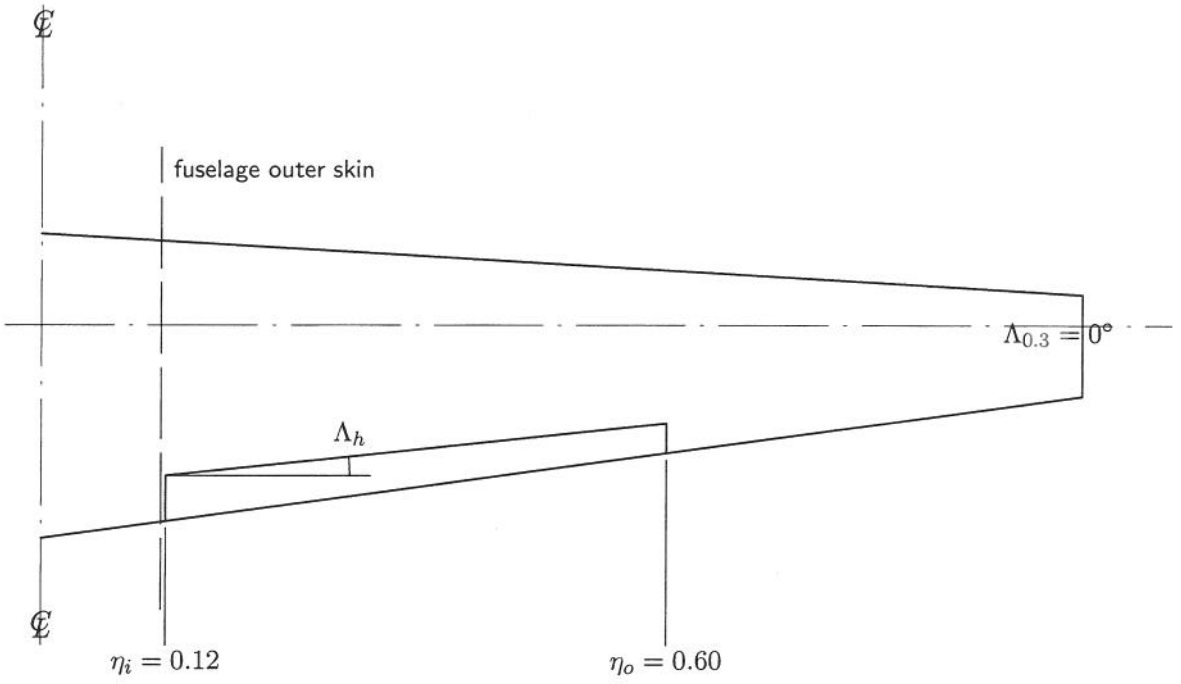


Figure A.1: Wing Geometry

## A.2 Mass Properties

### A.2.1 Fixed Structure

The empty fuselage, with no crew or passengers, has a mass of 3975 lb with the cg located at [202.3, 0, 0]. The moments of inertia about the body axes centre at [223, 0, 0] are:

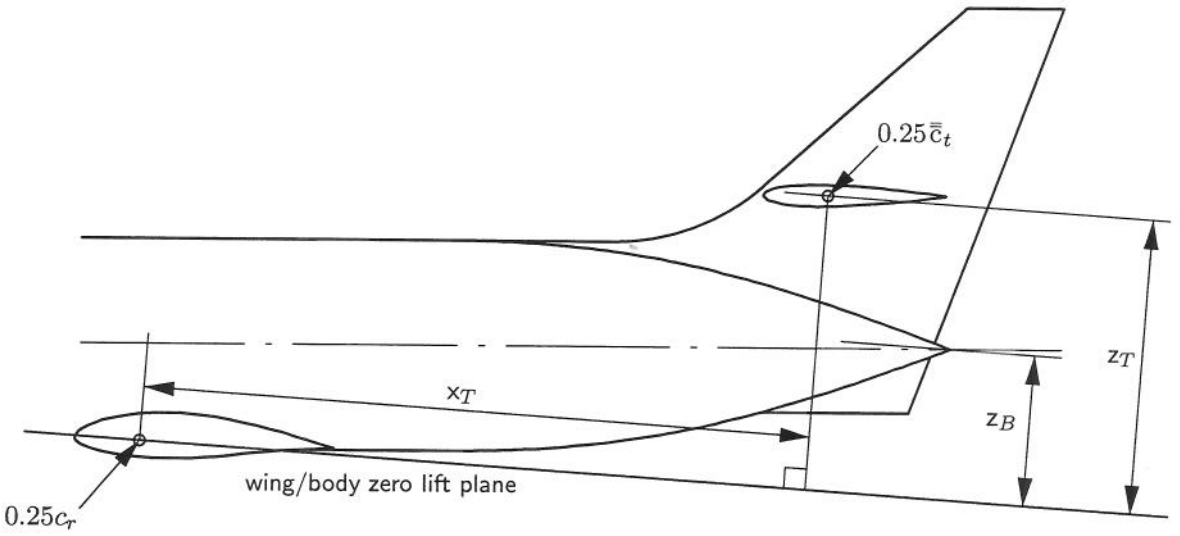


Figure A.2: Tailplane Location

$(I_{xx})_f =$ 6046127 lb.in$^2$
$(I_{yy})_f =$ 55297854 lb.in$^2$
$(I_{zz})_f =$ 55297854 lb.in$^2$

The wing has a mass of 2090 lb with the cg located at [228.5, 0, 24.4]. The moments and products of inertia are:

$(I_{xx})_w =$ 34066713 lb.in$^2$
$(I_{yy})_w =$ 1524258 lb.in$^2$
$(I_{zz})_w =$ 32733657 lb.in$^2$
$(I_{xz})_w =$ -261511 lb.in$^2$

Other parts of the aircraft are assumed to be point masses, located as follows:

| Item | Mass (lb) | CG Location up | CG Location down |
|---|---|---|---|
| Nose Undercarriage | 147 | [34.0, 0.0, 24.0] | [61.0, 0.0, 54.0] |
| Main Undercarriage | 221 | [241.2, 72.0, 26.8] | [ 243.5, 109.6, 52.2] |
| Main Undercarriage | 221 | [241.2, -72.0, 26.8] | [ 243.5, -109.6, 52.2] |
| Tail Unit | 588 | [474.9, 0.0, -53.0] | |
| Engine | 705 | [168.1, 105.3, 10.1] | |
| Engine | 705 | [168.1, -105.3, 10.1] | |

Table A.1: Location of Main Components

### A.2.2 Variable Masses

The passengers and crew are situated at fixed locations within the fuselage as indicated by the seat positions given in Table A.2. The fuel is stored in a set of wing tanks of rather complex shape. However the Type Record for the aircraft gives a tank-by-tank breakdown for

| Seat | Location |
|---|---|
| Pilot | [111.0, +15.60, 8.36] |
| Copilot | [111.0, -15.60, 8.36] |
| Attendant | [376.0, 0, 0] |
| 1A | [152.7, -22.48, +2.61] |
| 1B | [152.7, +6.88, +2.61] |
| 1C | [152.7, +22.48, +2.61] |
| 2A | [182.7, -22.48, +2.61] |
| 2B | [182.7, +6.88, +2.61] |
| 2C | [182.7, +22.48, +2.61] |
| 3A | [212.7, -22.48, +2.61] |
| 3B | [212.7, +6.88, +2.61] |
| 3C | [212.7, +22.48, +2.61] |
| 4A | [242.7, -22.48, +2.61] |
| 4B | [251.7, +6.88, +2.61] |
| 4C | [251.7, +22.48, +2.61] |
| 5A | [272.7, -22.48, +2.61] |
| 5B | [281.7, +6.88, +2.61] |
| 5C | [281.7, +22.48, +2.61] |
| 6A | [302.7, -22.48, +2.61] |
| 6B | [311.7, +6.88, +2.61] |
| 6C | [311.7, +22.48, +2.61] |

Table A.2: Seating Positions

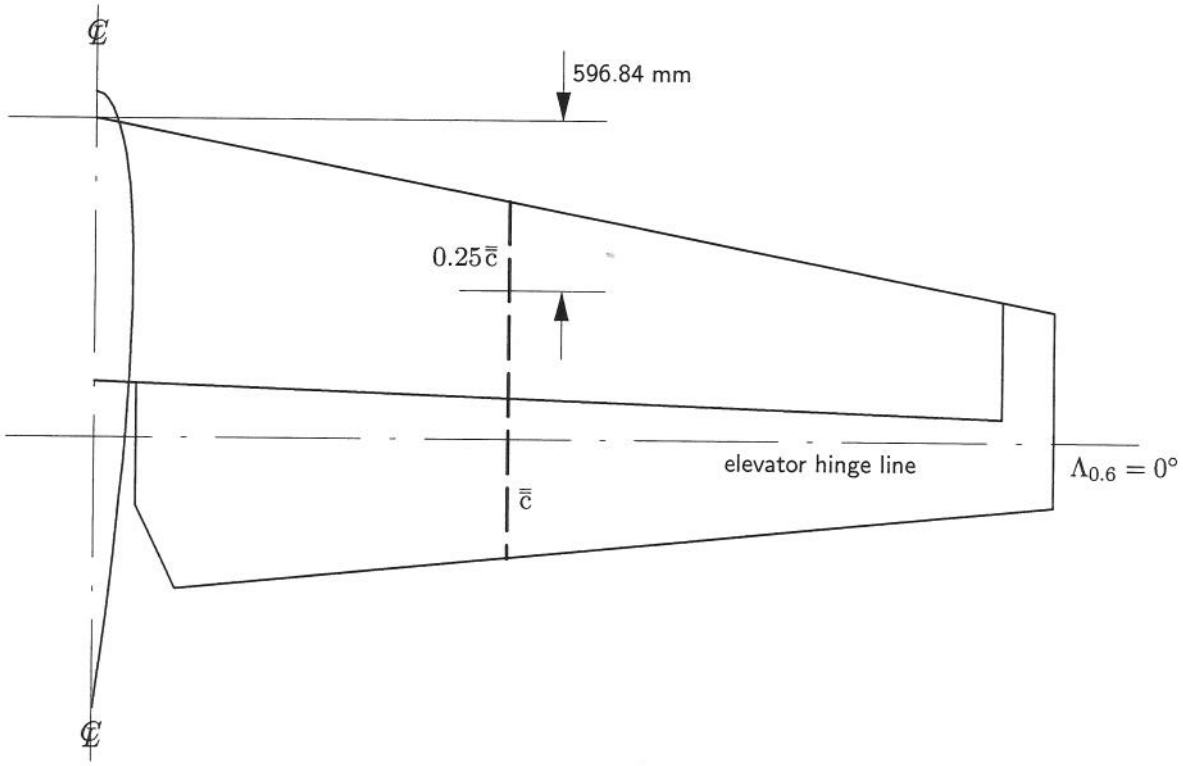


Figure A.3: Tailplane Geometry

the maximum weight configuration, see Table A.3. Using this data the variation in cg location and inertia can be determined as function of fuel mass as shown in Table

| Mass (lb) | Location |
|---|---|
| 52.0 | [214.3, 51.0, 30.3] |
| 97.0 | [214.7, 67.0, 28.3] |
| 114.7 | [218.5, 83.0, 26.4] |
| 134.5 | [221.8, 99.0, 24.4] |
| 169.2 | [227.6, 115.0, 22.4] |
| 193.4 | [230.6, 133.0, 20.2] |
| 168.6 | [230.2, 151.0, 18.0] |
| 147.2 | [229.8, 169.0, 15.8] |
| 128.4 | [229.4, 187.0, 13.6] |
| 109.8 | [229.0, 205.0, 11.4] |
| 88.5 | [228.6, 223.0, 9.2] |
| 64.2 | [228.4, 241.0, 7.0] |
| 42.7 | [228.2, 259.0, 4.8] |
| 22.9 | [228.1, 277.0, 2.6] |
| 2.9 | [227.9, 295.0, 0.3] |

Table A.3: Location of Fuel Masses - per wing

| Fuel Mass (lb) | CG Position | $I_{xx}$ (lb.in$^2$) | $I_{yy}$ (lb.in$^2$) | $I_{zz}$ (lb.in$^2$) | $I_{xz}$ (lb.in$^2$) |
|---|---|---|---|---|---|
| 104.0 | [214.3, 0.0, 30.3] | 366036 | 103403 | 278376 | 27423 |
| 298.0 | [214.6, 0.0, 29.0] | 1392752 | 272618 | 1162606 | 73061 |
| 527.4 | [216.3, 0.0, 27.9] | 3132715 | 436890 | 2747588 | 100292 |
| 796.4 | [218.1, 0.0, 26.7] | 5929524 | 597618 | 5384445 | 108173 |
| 1134.8 | [221.0, 0.0, 25.4] | 10575415 | 775329 | 9866945 | 73227 |
| 1521.6 | [223.4, 0.0, 24.1] | 17575971 | 956121 | 16731392 | 13729 |
| 1858.8 | [224.6, 0.0, 23.0] | 25374079 | 1083213 | 24437370 | -30044 |
| 2153.2 | [225.3, 0.0, 22.0] | 33856112 | 1170501 | 32859341 | -61713 |
| 2410.0 | [225.8, 0.0, 21.1] | 42883714 | 1228582 | 41849899 | -84080 |
| 2629.6 | [226.0, 0.0, 20.3] | 52140939 | 1265023 | 51086494 | -99100 |
| 2806.6 | [226.2, 0.0, 19.6] | 60957918 | 1285519 | 59894078 | -108208 |
| 2935.0 | [226.3, 0.0, 19.1] | 68421772 | 1295517 | 67355423 | -113047 |
| 3020.4 | [226.4, 0.0, 18.7] | 74152432 | 1299768 | 73086449 | -115165 |
| 3066.2 | [226.4, 0.0, 18.4] | 77666920 | 1301259 | 76601829 | -115762 |
| 3072.0 | [226.4, 0.0, 18.4] | 78171665 | 1301399 | 77106713 | -115772 |

Table A.4: Fuel Load - CG Location and Inertias

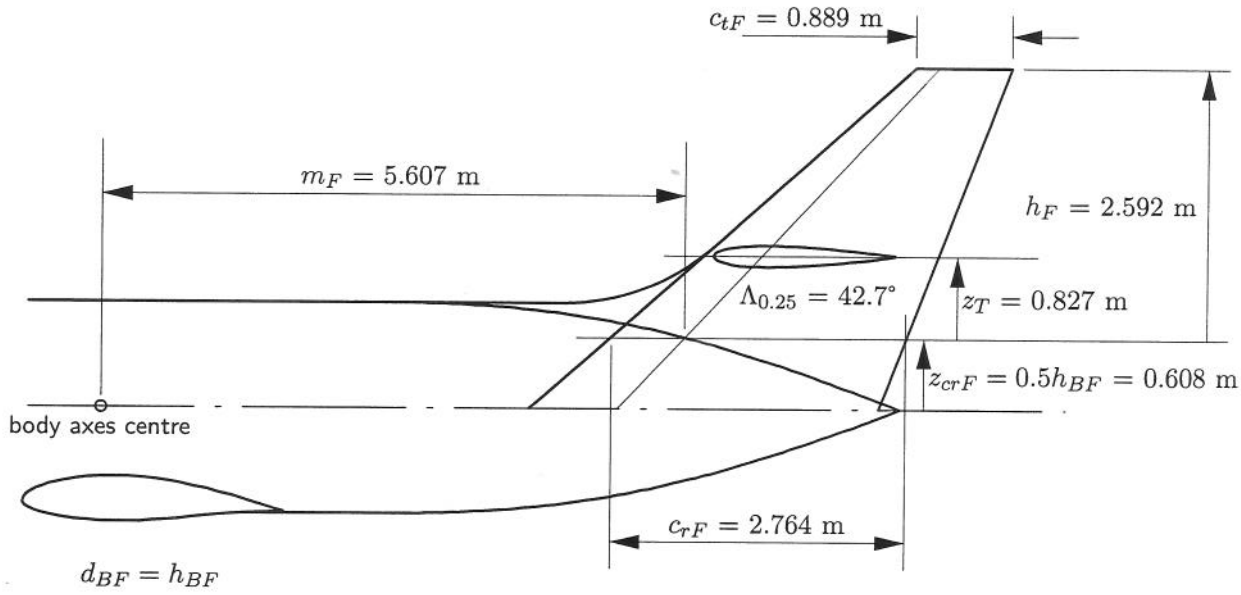


Figure A.4: Fin Geometry

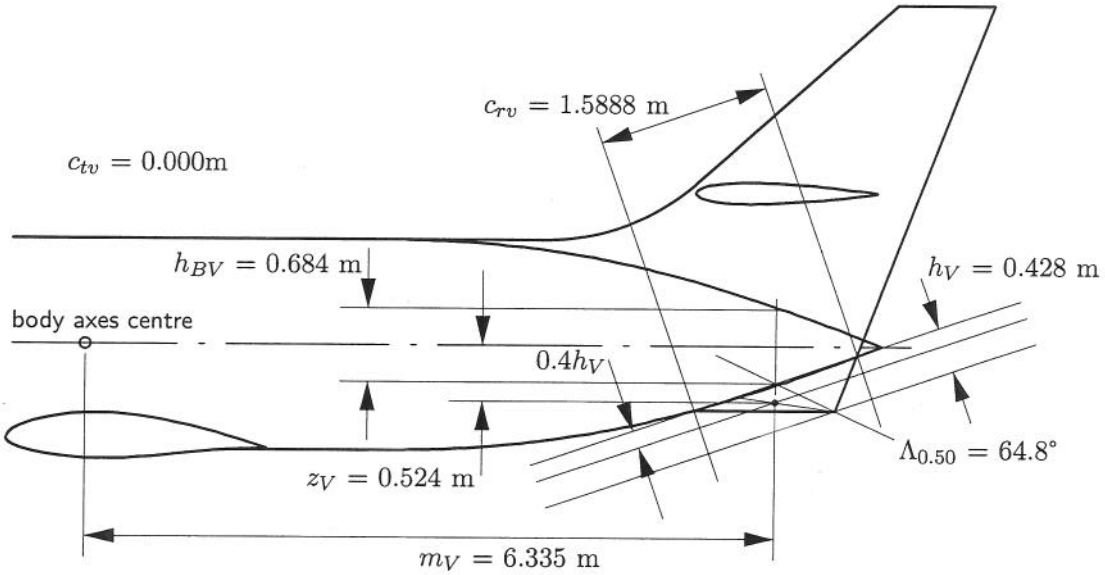


(aero-centre of fin based on quarter chord) $d_{BV} = h_{BV}$

Figure A.5: Ventral Fin Geometry

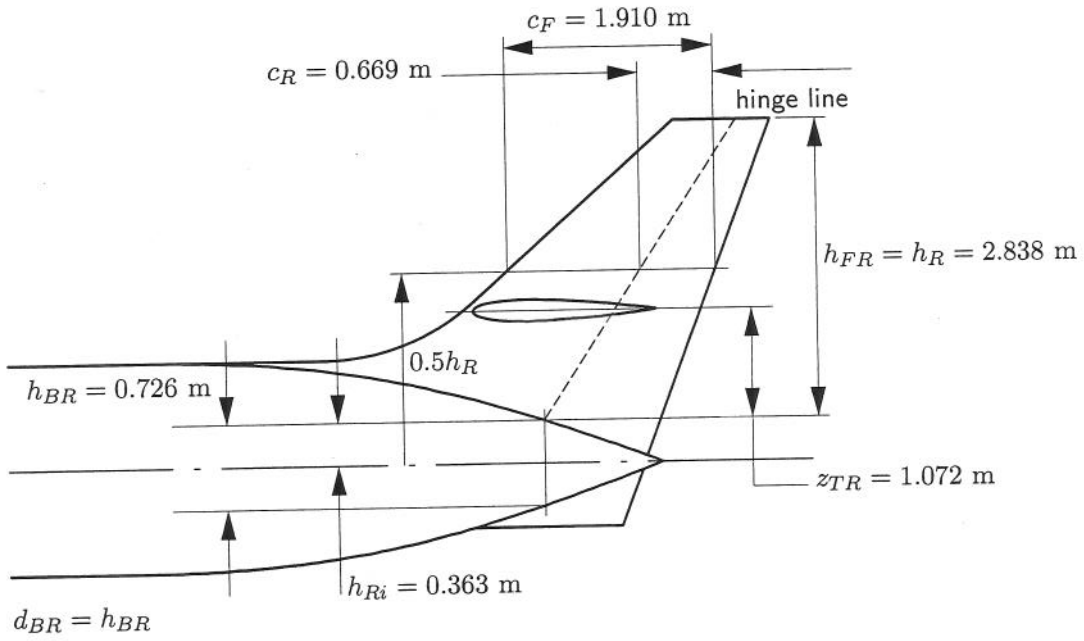


Figure A.6: Simplified Rudder Geometry

# Appendix B

# Aerofoil Data

## B.1 NACA 63A418

Using the method given in ESDU 72024 the following section parameters were determined from Table B.1 for inviscid compressible flow assuming sub-critical Mach numbers. Viscous flow effects were estimated using ESDU 97020 and the average Reynolds numbers given in Table 1.3.

$$\frac{t}{c} = 0.180 \quad \frac{2z_{t_1}}{t} = 0.154 \quad \frac{2z_{t_2}}{t} = 0.479 \quad \frac{x_t}{c} = 0.35 \quad \tau_a = 20.1^\circ \quad \tan\left(\frac{\tau_a}{2}\right) = 0.177$$

$$\frac{h+}{c} = \frac{z_{c4}}{c} = 0.0266 \quad \frac{z_{c_2}}{h+} = 0.346 \quad \frac{z_{c_3}}{z_{c_4}} = 0.722 \quad \frac{z_{c_6}}{z_{c_4}} = 0.304$$

$$\frac{z_{c_5}}{h+} = 0.380 \quad \frac{z_{c_2}}{h+} = 0.346 \quad \tan\tau_{au} = 0.278 \quad C_{M_{0_i}} = -0.0877$$

Which leads to the estimates given in Table B.2. The variation of zero-lift angle of attack, $\alpha_0$, with Mach number and Reynolds number was obtained using ESDU 98011, noting that $\log_{10}(z_{c_6}/z_{c_4}) = \log_{10}(0.304) = -0.517$ and that $(\alpha_0)_T = -0.05565$ rad, see also Table B.2.

## B.2 NACA 63A412

Using the method given in ESDU 72024 the following section parameters were determined from Table B.3 for inviscid compressible flow assuming sub-critical Mach numbers. Viscous flow effects were estimated using ESDU 97020 and the average Reynolds numbers given in Table 1.3.

$$\frac{t}{c} = 0.120 \quad \frac{2z_{t_1}}{t} = 0.165 \quad \frac{2z_{t_2}}{t} = 0.485 \quad \frac{x_t}{c} = 0.35 \quad \tau_a = 13.8^\circ \quad \tan\left(\frac{\tau_a}{2}\right) = 0.121$$

$$\frac{h+}{c} = \frac{z_{c4}}{c} = 0.0266 \quad \frac{z_{c_2}}{h+} = 0.304 \quad \frac{z_{c_3}}{z_{c_4}} = 0.709 \quad \frac{z_{c_6}}{z_{c_4}} = 0.299 \quad \alpha_{0_i} = -0.0586 \text{ rad}$$

$$\frac{z_{c_5}}{h+} = 0.374 \quad \frac{z_{c_2}}{h+} = 0.304 \quad \tan\tau_{au} = 0.220 \quad C_{M_{0_i}} = -0.0891$$

Which leads to the estimates given in Table B.4. The variation of zero-lift angle of attack, $\alpha_0$, with Mach number and Reynolds number was obtained using ESDU 98011, noting that $\log_{10}(z_{c_6}/z_{c_4}) = \log_{10}(0.299) = -0.524$ and that $(\alpha_0)_T = -0.05483$ rad, see also Table B.4.

## B.3 NACA 0012

Using the method given in ESDU 72024 the following section parameters were determined from Table B.5 for inviscid compressible flow assuming sub-critical Mach numbers. Viscous flow effects were estimated using ESDU 97020 and the average Reynolds numbers given in Table 1.3.

$$\frac{t}{c} = 0.120 \quad \frac{2z_{t_1}}{t} = 0.204 \quad \frac{2z_{t_2}}{t} = 0.592 \quad \frac{x_t}{c} = 0.30 \quad \tau = 16.0^\circ \quad \tan\left(\frac{\tau_a}{2}\right) = 0.140$$

Which leads to the estimates given in Table B.6.

## B.4 NACA 0010

Using the method given in ESDU 72024 the following section parameters were determined from Table B.7 for inviscid compressible flow assuming sub-critical Mach numbers. Viscous flow effects were estimated using ESDU 97020 and the average Reynolds numbers given in Table 1.3.

$$\frac{t}{c} = 0.100 \quad \frac{2z_{t_1}}{t} = 0.204 \quad \frac{2z_{t_2}}{t} = 0.592 \quad \frac{x_t}{c} = 0.30 \quad \tau = 13.3^\circ \quad \tan\left(\frac{\tau_a}{2}\right) = 0.117$$

Which leads to the estimates given in Table B.8.

| Upper Surface Station | Upper Surface Ordinate | Lower Surface Station | Lower Surface Ordinate | x/c | $z_t/c$ | $z_c/c$ |
|---|---|---|---|---|---|---|
| 0.00 | 0.0000 | 0.00 | 0.0000 | 0.0000 | 0.00000 | 0.00000 |
| 0.50 | 1.8124 | 0.50 | -0.9616 | 0.0050 | 0.01387 | 0.00425 |
| 0.75 | 2.1365 | 0.75 | -1.2213 | 0.0075 | 0.01679 | 0.00458 |
| 1.25 | 2.6889 | 1.25 | -1.6157 | 0.0125 | 0.02152 | 0.00537 |
| 2.50 | 3.7234 | 2.50 | -2.3864 | 0.0250 | 0.03055 | 0.00669 |
| 5.00 | 5.2337 | 5.00 | -3.3965 | 0.0500 | 0.04315 | 0.00919 |
| 7.50 | 6.3833 | 7.50 | -4.1141 | 0.0750 | 0.05249 | 0.01135 |
| 10.00 | 7.3247 | 10.00 | -4.6721 | 0.1000 | 0.05998 | 0.01326 |
| 15.00 | 8.7955 | 15.00 | -5.4915 | 0.1500 | 0.07144 | 0.01652 |
| 20.00 | 9.8798 | 20.00 | -6.0429 | 0.2000 | 0.07961 | 0.01918 |
| 25.00 | 10.6658 | 25.00 | -6.3919 | 0.2500 | 0.08529 | 0.02137 |
| 30.00 | 11.1884 | 30.00 | -6.565 | 0.3000 | 0.08877 | 0.02312 |
| 35.00 | 11.4514 | 35.00 | -6.5535 | 0.3500 | 0.09002 | 0.02449 |
| 40.00 | 11.4751 | 40.00 | -6.3712 | 0.4000 | 0.08923 | 0.02552 |
| 45.00 | 11.2711 | 45.00 | -6.0270 | 0.4500 | 0.08649 | 0.02622 |
| 50.00 | 10.8696 | 50.00 | -5.5534 | 0.5000 | 0.08212 | 0.02658 |
| 55.00 | 10.2947 | 55.00 | -4.9802 | 0.5500 | 0.07637 | 0.02657 |
| 60.00 | 9.5661 | 60.00 | -4.3309 | 0.6000 | 0.06949 | 0.02618 |
| 65.00 | 8.7015 | 65.00 | -3.6346 | 0.6500 | 0.06168 | 0.02533 |
| 70.00 | 7.7167 | 70.00 | -2.9224 | 0.7000 | 0.05320 | 0.02397 |
| 75.00 | 6.6379 | 75.00 | -2.2412 | 0.7500 | 0.04440 | 0.02198 |
| 80.00 | 5.4753 | 80.00 | -1.6473 | 0.8000 | 0.03561 | 0.01914 |
| 85.00 | 4.1705 | 85.00 | -1.1966 | 0.8500 | 0.02684 | 0.01487 |
| 90.00 | 2.8058 | 90.00 | -0.7830 | 0.9000 | 0.01794 | 0.01011 |
| 92.00 | 2.2558 | 92.00 | -0.6376 | 0.9200 | 0.01447 | 0.00809 |
| 95.00 | 1.4309 | 95.00 | -0.4195 | 0.9500 | 0.00925 | 0.00506 |
| 100.00 | 0.0295 | 100.00 | -0.0295 | 1.0000 | 0.00030 | 0.00000 |

Table B.1: Aerofoil Section - NACA 63A418

| Mach | $\log_{10} R_e$ | $a_{1_i}$ rad$^{-1}$ | $a_1/a_{1_i}$ | $C_{M_0}$ | $k_v$ | $k_M$ | $\alpha_0$ rad |
|---|---|---|---|---|---|---|---|
| 0.05 | 6.24 | 7.194 | 0.906 | -0.0878 | 0.865 | 0.999 | -0.04806 |
| 0.10 | 6.54 | 7.236 | 0.919 | -0.0882 | 0.885 | 0.998 | -0.04915 |
| 0.15 | 6.72 | 7.298 | 0.925 | -0.0887 | 0.895 | 0.997 | -0.04966 |
| 0.20 | 6.84 | 7.379 | 0.929 | -0.0895 | 0.903 | 0.996 | -0.05004 |
| 0.25 | 6.94 | 7.482 | 0.931 | -0.0906 | 0.908 | 0.994 | -0.05023 |
| 0.30 | 7.02 | 7.614 | 0.932 | -0.0920 | 0.911 | 0.993 | -0.05031 |
| 0.35 | 7.08 | 7.772 | 0.932 | -0.0936 | 0.914 | 0.990 | -0.05037 |
| 0.40 | 7.14 | 7.985 | 0.932 | -0.0957 | 0.917 | 0.987 | -0.05039 |
| 0.45 | 7.19 | 8.262 | 0.930 | -0.0982 | 0.920 | 0.984 | -0.05035 |
| 0.50 | 7.24 | 8.650 | 0.928 | -0.1013 | 0.922 | 0.978 | -0.05016 |
| 0.55 | 7.28 | 9.223 | 0.924 | -0.1050 | 0.924 | 0.970 | -0.04985 |

Table B.2: Aerodynamic Estimates - NACA 63A418

| Upper Surface Station | Upper Surface Ordinate | Lower Surface Station | Lower Surface Ordinate | x/c | $z_t/c$ | $z_c/c$ |
|---|---|---|---|---|---|---|
| 0.00 | 0.0000 | 0.00 | 0.0000 | 0.0000 | 0.00000 | 0.00000 |
| 0.50 | 1.2647 | 0.50 | -0.7125 | 0.0050 | 0.00989 | 0.00276 |
| 0.75 | 1.4942 | 0.75 | -0.8825 | 0.0075 | 0.01188 | 0.00306 |
| 1.25 | 1.8867 | 1.25 | -1.1350 | 0.0125 | 0.01511 | 0.00376 |
| 2.50 | 2.6269 | 2.50 | -1.5634 | 0.0250 | 0.02095 | 0.00532 |
| 5.00 | 3.7192 | 5.00 | -2.1042 | 0.0500 | 0.02912 | 0.00808 |
| 7.50 | 4.5622 | 7.50 | -2.4761 | 0.0750 | 0.03519 | 0.01043 |
| 10.00 | 5.2592 | 10.00 | -2.7571 | 0.1000 | 0.04008 | 0.01251 |
| 15.00 | 6.3600 | 15.00 | -3.1579 | 0.1500 | 0.04759 | 0.01601 |
| 20.00 | 7.1822 | 20.00 | -3.4105 | 0.2000 | 0.05296 | 0.01886 |
| 25.00 | 7.7886 | 25.00 | -3.5530 | 0.2500 | 0.05671 | 0.02118 |
| 30.00 | 8.2107 | 30.00 | -3.6028 | 0.3000 | 0.05907 | 0.02304 |
| 35.00 | 8.4477 | 35.00 | -3.5504 | 0.3500 | 0.05999 | 0.02449 |
| 40.00 | 8.5152 | 40.00 | -3.4041 | 0.4000 | 0.05960 | 0.02556 |
| 45.00 | 8.4193 | 45.00 | -3.1678 | 0.4500 | 0.05794 | 0.02626 |
| 50.00 | 8.1779 | 50.00 | -2.8590 | 0.5000 | 0.05518 | 0.02659 |
| 55.00 | 7.8035 | 55.00 | -2.4941 | 0.5500 | 0.05149 | 0.02655 |
| 60.00 | 7.3107 | 60.00 | -2.0911 | 0.6000 | 0.04701 | 0.02610 |
| 65.00 | 6.7073 | 65.00 | -1.6673 | 0.6500 | 0.04187 | 0.02520 |
| 70.00 | 6.0038 | 70.00 | -1.2436 | 0.7000 | 0.03624 | 0.02380 |
| 75.00 | 5.2073 | 75.00 | -0.8514 | 0.7500 | 0.03029 | 0.02178 |
| 80.00 | 4.3224 | 80.00 | -0.5415 | 0.8000 | 0.02432 | 0.01890 |
| 85.00 | 3.2952 | 85.00 | -0.3696 | 0.8500 | 0.01832 | 0.01463 |
| 90.00 | 2.2251 | 90.00 | -0.2354 | 0.9000 | 0.01230 | 0.00995 |
| 92.00 | 1.7847 | 92.00 | -0.1929 | 0.9200 | 0.00989 | 0.00796 |
| 95.00 | 1.1241 | 95.00 | -0.1291 | 0.9500 | 0.00627 | 0.00498 |
| 100.00 | 0.0188 | 100.00 | -0.0188 | 1.0000 | 0.00019 | 0.00000 |

Table B.3: Aerofoil Section - NACA 63A412

| Mach | $\log_{10} R_e$ | $a_{1_i}$ rad$^{-1}$ | $a_1/a_{1_i}$ | $C_{M_0}$ | $k_v$ | $k_M$ | $\alpha_0$ rad |
|---|---|---|---|---|---|---|---|
| 0.05 | 6.13 | 6.889 | 0.925 | -0.0892 | 0.860 | 0.998 | -0.05454 |
| 0.10 | 6.43 | 6.930 | 0.933 | -0.0895 | 0.873 | 0.998 | -0.05442 |
| 0.15 | 6.61 | 6.988 | 0.938 | -0.0901 | 0.883 | 0.996 | -0.05422 |
| 0.20 | 6.73 | 7.066 | 0.941 | -0.0909 | 0.891 | 0.995 | -0.05402 |
| 0.25 | 6.83 | 7.164 | 0.943 | -0.0920 | 0.898 | 0.994 | -0.05374 |
| 0.30 | 6.91 | 7.288 | 0.944 | -0.0934 | 0.904 | 0.992 | -0.05346 |
| 0.35 | 6.98 | 7.437 | 0.945 | -0.0951 | 0.909 | 0.989 | -0.05298 |
| 0.40 | 7.03 | 7.624 | 0.944 | -0.0972 | 0.913 | 0.986 | -0.05250 |
| 0.45 | 7.09 | 7.857 | 0.943 | -0.0998 | 0.916 | 0.982 | -0.05175 |
| 0.50 | 7.13 | 8.158 | 0.942 | -0.1029 | 0.918 | 0.977 | -0.05100 |
| 0.55 | 7.17 | 8.561 | 0.934 | -0.1067 | 0.919 | 0.969 | -0.04968 |

Table B.4: Aerodynamic Estimates - NACA 63A412

| Station | Ordinate | x/c | $z_t/c$ |
|---|---|---|---|
| 0.00 | 0.0000 | 0.0000 | 0.0000 |
| 0.50 | 1.2213 | 0.0050 | 0.0122 |
| 0.75 | 1.4849 | 0.0075 | 0.0148 |
| 1.25 | 1.8939 | 0.0125 | 0.0189 |
| 2.50 | 2.6147 | 0.0250 | 0.0261 |
| 5.00 | 3.5547 | 0.0500 | 0.0355 |
| 7.50 | 4.1999 | 0.0750 | 0.0420 |
| 10.00 | 4.6828 | 0.1000 | 0.0468 |
| 15.00 | 5.3452 | 0.1500 | 0.0535 |
| 20.00 | 5.7375 | 0.2000 | 0.0574 |
| 25.00 | 5.9412 | 0.2500 | 0.0594 |
| 30.00 | 6.0017 | 0.3000 | 0.0600 |
| 35.00 | 5.9486 | 0.3500 | 0.0595 |
| 40.00 | 5.8030 | 0.4000 | 0.0580 |
| 45.00 | 5.5807 | 0.4500 | 0.0558 |
| 50.00 | 5.2940 | 0.5000 | 0.0529 |
| 55.00 | 4.9524 | 0.5500 | 0.0495 |
| 60.00 | 4.5634 | 0.6000 | 0.0456 |
| 65.00 | 4.1325 | 0.6500 | 0.0413 |
| 70.00 | 3.6639 | 0.7000 | 0.0366 |
| 75.00 | 3.1603 | 0.7500 | 0.0316 |
| 80.00 | 2.6231 | 0.8000 | 0.0262 |
| 85.00 | 2.0526 | 0.8500 | 0.0205 |
| 90.00 | 1.4477 | 0.9000 | 0.0145 |
| 92.00 | 1.1913 | 0.9200 | 0.0119 |
| 95.00 | 0.8066 | 0.9500 | 0.0081 |
| 100.00 | 0.126 | 1.0000 | 0.0013 |

Table B.5: Aerofoil Section - NACA 0012

| Mach | 0.05 | 0.10 | 0.15 | 0.20 | 0.25 | 0.30 | 0.35 | 0.40 | 0.45 | 0.50 | 0.55 |
|---|---|---|---|---|---|---|---|---|---|---|---|
| $\log_{10} R_e$ | 6.23 | 6.54 | 6.71 | 6.84 | 6.93 | 7.01 | 7.08 | 7.14 | 7.19 | 7.23 | 7.28 |
| $a_{1_i}$ | 6.915 | 6.956 | 7.015 | 7.093 | 7.191 | 7.314 | 7.463 | 7.648 | 7.875 | 8.163 | 8.539 |
| $a_1/a_{1_i}$ | 0.925 | 0.933 | 0.939 | 0.941 | 0.942 | 0.943 | 0.944 | 0.944 | 0.943 | 0.942 | 0.941 |

Table B.6: Aerodynamic Estimates - NACA 0012

| Station | Ordinate | x/c | $z_t/c$ |
|---|---|---|---|
| 0.00 | 0.0000 | 0.0000 | 0.0000 |
| 0.50 | 1.0178 | 0.0050 | 0.0102 |
| 0.75 | 1.2374 | 0.0075 | 0.0124 |
| 1.25 | 1.5783 | 0.0125 | 0.0158 |
| 2.50 | 2.1789 | 0.0250 | 0.0218 |
| 5.00 | 2.9622 | 0.0500 | 0.0296 |
| 7.50 | 3.4999 | 0.0750 | 0.0350 |
| 10.00 | 3.9023 | 0.1000 | 0.0390 |
| 15.00 | 4.4543 | 0.1500 | 0.0445 |
| 20.00 | 4.7813 | 0.2000 | 0.0478 |
| 25.00 | 4.9510 | 0.2500 | 0.0495 |
| 30.00 | 5.0014 | 0.3000 | 0.0500 |
| 35.00 | 4.9572 | 0.3500 | 0.0496 |
| 40.00 | 4.8358 | 0.4000 | 0.0484 |
| 45.00 | 4.6506 | 0.4500 | 0.0465 |
| 50.00 | 4.4117 | 0.5000 | 0.0441 |
| 55.00 | 4.1270 | 0.5500 | 0.0413 |
| 60.00 | 3.8028 | 0.6000 | 0.0380 |
| 65.00 | 3.4437 | 0.6500 | 0.0344 |
| 70.00 | 3.0533 | 0.7000 | 0.0305 |
| 75.00 | 2.6336 | 0.7500 | 0.0263 |
| 80.00 | 2.1859 | 0.8000 | 0.0219 |
| 85.00 | 1.7105 | 0.8500 | 0.0171 |
| 90.00 | 1.2064 | 0.9000 | 0.0121 |
| 92.00 | 0.9927 | 0.9200 | 0.0099 |
| 95.00 | 0.6721 | 0.9500 | 0.0067 |
| 100.00 | 0.1050 | 1.0000 | 0.0011 |

Table B.7: Aerofoil Section - NACA 0010

| Mach | 0.05 | 0.10 | 0.15 | 0.20 | 0.25 | 0.30 | 0.35 | 0.40 | 0.45 | 0.50 | 0.55 |
|---|---|---|---|---|---|---|---|---|---|---|---|
| $\log_{10} R_e$ | 5.79 | 6.09 | 6.27 | 6.39 | 6.49 | 6.57 | 6.64 | 6.70 | 6.75 | 6.79 | 6.83 |
| $a_{1_i}$ | 6.819 | 6.859 | 6.917 | 6.994 | 7.092 | 7.213 | 7.359 | 7.539 | 7.759 | 8.034 | 8.386 |
| $a_1/a_{1_i}$ | 0.924 | 0.934 | 0.938 | 0.941 | 0.943 | 0.944 | 0.945 | 0.945 | 0.944 | 0.943 | 0.941 |

Table B.8: Aerodynamic Estimates - NACA 0010